Dissertation

Master in Automotive Engineering

Thermal energy recovery systems for automotive vehicles: swashplate expander modeling

Vitor Manuel Cerqueira Magro Lopes

Leiria, *september* of 2015

Dissertation

Master in Automotive Engineering

Thermal energy recovery systems for automotive vehicles: swashplate expander modeling

Vitor Manuel Cerqueira Magro Lopes

Dissertation of Master developed under the supervision of Professor Hélder Manuel Ferreira Santos, Professor at *School of Technology and Management of the Polytecnic Institute of Leiria*, and co-supervision of Professor João Francisco Romeiro da Fonseca Pereira.

Leiria, *september* of *2015*

This page was intetionally left blank

Acknowledgements

The first thank goes to my mentor, Professor Hélder Santos, for all the support, patience, enthusiasm and interest and during all the steps of the work, giving me extra motivation. His advices and suggestions were very helpful in crucial phases and in some decisions that needed to be made throughout, and his knowledge was a benefit for the overall project. I also thank to Professor João Fonseca Pereira for the help and support throughout the development of the project.

Secondly, I thank a lot to my co mentor Vicente Dolz. I am very grateful for the opportunity that was given to me by him, by accepting me and mentoring me in the CMT-*Centro de Motores Térmicos*. His knowledge in the matter was very helpful and I feel I learned a lot in the matter of the ORC systems during my internship year. All the knowledge acquired there was fundamental for this work: theory, logic, software usage and experimental runs. It was a really great opportunity that was conceded to me.

A big thank goes to my colleague Lucía Royo for all the help, support, for encouraging me and for being such a good coworker; I also thank to Petar Kleut for making me feel like home, to Jaime Sánchez, Luís Miguel, Paula, Ana and Teresa.

Another acknowledgement goes to my colleague André Almeida for his advices and support.

I also thank to my parents Vitor and Aida, and my sister Ana for all their support and advices and for believing in me no matter what, and for encouraging me to go all the way and never give up.

This page was intetionally left blank

Resumo

No ínicio deste trabalho, foram abordadas algumas questões. O primeiro passo no desenvolvimento do presente estudo consiste numa extensa revisão literária acerca de sistemas de recuperação de energia térmica em veículos automóveis. A revisão literária foi essencial para identificar o ciclo de Rankine como uma solução de elevado potencial para aplicação em veículos. Foi desenvolvida e apresentada uma metodologia que permite determinar que tipo de expanser é mais adequado para um dado sistema com ciclo de Rankine, utilizando o diagrama NsDs. Os parametros que têm influência na seleção do expansor são: o fluido de trabalho, as condições de entrada e de saída (temperatura, pressão, tipo de fluido e caudal mássico), a velocidade de rotação e o diâmetro do expansor. O caudal mássico é calculado de acordo com o intervalo de potência normalmente obtido através do evaporador instalado em veículos automóveis (de 10 kW a 500 kW). O presente trabalho apresenta uma metodologia que permite a seleção do expansor para uma dada aplicação. Para isso, foram selecionados três fluidos de trabalho (R245fa, etanol e água) para demonstrar a metodologia desenvolvida. O modelo desenvolvido em AMESim foi validado e comparado com resultados obtidos experimentalmente, que confirmaram a precisão dos mesmos.

Palavras-chave: *Sistemas de recuperação de energia térmica, Ciclo de Rankine, Seleção do Expansor, Fluidos de trabalho, desenvolvimento de um modelo*

This page was intetionally left blank

Abstract

At the beginning of this work, a number of issues had to be addressed. A first step in the development of the present study consists on the extensive literature review on the automotive vehicle waste heat recovery systems. The literature review was essential to identify the Rankine cycle as a high potential solution for vehicle applications. A methodology was developed and presented in order to determine which type of expander suits best in a given RC system, using the NsDs turbine chart. The parameters that have influence on the expander's selection are: the working fluid inlet and outlet conditions (such as the temperature, pressure, type of fluid and the mass flow rate), the rotating speed and the diameter of the expander. The mass flow rate will be calculated according to the usual power extracted by the evaporator from waste heat recovery systems installed in automotive vehicles (10 kW to 500 kW). The present work presents a methodology that allows selecting an expander for a specific application. To this end, three different working fluids (R245fa, ethanol and water) were selected to demonstrate the developed methodology. The model developed in AMESim was validated by comparing the results with the ones obtained through experimental runs, which confirmed its accuracy in the results obtained.

Keywords: *Waste heat recovery, Rankine cycle, Expander selection, Working fluids, Model development*

This page was intetionally left blank

List of figures

List of tables

This page was intetionally left blank

List of acronyms

Latin Characters

a	speed of sound (340,29 [m/s])
C	isentropic spouting velocity [m/s]
Cp	specific heat at constant pressure [kJ/kg.K]
cte	constant [-]
D	diameter [m]
g	acceleration of gravity $[\mathrm{m/s^2}]$
H	height [ft] or [m]
h	specific enthalpy [kJ/kg]
$\dot{m}$	mass flow rate [kg/s]
N	rotary speed [rpm]
P	pressure [Pa]
$\dot{Q}$	thermal power [W]
Re	Reynolds number [-]
s	specific entropy [kJ/kg.K]
T	temperature [ºC] or [K]
U	tip speed [m/s]
$\dot{V}$	volumetric flow rate $[\mathrm{m^3/s}]$
W	work [J]

Greek Characters

Δ	differential
η	efficiency [-]
Π	pressure ratio [-]
ρ	density $[\mathrm{m^3/kg}]$
υ	kinematic viscosity $[\mathrm{m^2/s}]$
Φ	flow coefficient (for Japikse's chart) [-]
Ψ	head coefficient (for Japilse's chart) [-]

Subscripts

amb	ambient
$cond$	condenser
$evap$	evaporator
ex	exhaust
in	inlet
$loss$	loss
$mech$	mechanical
$mech, exp$	mechanical expander
out	outlet
$pump$	pump
s	isentropic
su	supply
t	turbine
th	thermal

Abbreviations

1D	One-dimensional
3D	Three-dimensional
BC	Bottoming Cycle
BDC	Bottom Dead Center
CAD	Computer aided design
EES	Engineering Equation Solver
EGR	Exhaust Gas Recirculation
ETC	Electric Turbo-Compounding
FEM	Finite Element Method
GWP	Global Warming Potential
HD	Heavy Duty
HDD	Heavy Duty Diesel
HT	High-temperature
ICE	Internal Combustion Engine
IFP	*Institut Français du Pétrole* (French Institute of Petrol)

ISO	International Organization for Standardization
LCA	Life-cycle assessment
LiIon	Lithium-ion
LT	Low-temperature
MTC	Mechanical Turbo-Compounding
NFPA	National Fire Protection Association
NIST	National Institute of Standards and Technology
NPSS	Numerical Propulsion System Simulation
ODP	Ozone Depletion Potential
ORC	Organic Rankine Cycle
PPTD	Pinch Point Temperature Difference
PV	Pressure-volume
RC	Rankine Cycle
rpm	Rotation per minute
SI	*Système International d'Unités* (International System of Units)
TIGERS	Turbo-Generator Integrated Gas Energy Recovery System
TDC	Top Dead Center
VFR	Volume flow ratio
WHR	Waste Heat Recovery

This page was intetionally left blank

Table of contents

1. Introduction

1.1. Motivation

Two thirds of the total fuel energy consumed by Internal Combustion Engine (ICE) is wasted by the cooling circuit and the exhaust. Therefore, if some part of this energy can be recovered and converted into useful (mechanical or electric) energy, the overall efficiency of the automotive could be raised and the fuel consumption could be lowered. Many studies have been performed, particularly on the Organic Rankine cycle (ORC), for the recovery of the heat energy wasted by the exhaust gases. One of the key components of this system is the expansion machine, which has a strong impact on the cycle's performance. Many expanders have been theoretically studied and simulated, by the means of softwares and real runs, but only few studies on the reciprocating piston expander as an expansion machine have been performed until the present. As a result, the present study approaches the general ORC system with special attention to the expander machine.

1.2. Goals and Outline

The aim of this work is to study and model a swash plate piston expander in the engineering software AMESim. The main goal is to develop a modelation that will be calibrated with experimental data, so that, in the future, expensive experimental tests can be avoided. To achieve this main goal, the present work addresses the following issues:

- Literature review on the ORC for automotive vehicle applications, its components and the working fluids;

- Describe with detail the expansion process, review the existing expanders and explain which type of expander is best for a determined application;

- Study the AMESim interface, libraries and how to model an engineering system, which data can be input and obtained and how to run and extract the results;

- Model the expander and perform a series of runs with the experimental data in order to adjust and calibrate the final model.

1.3. General Contents

This work is organized in five chapters. The chapter 1 introduces the subject of the present work, explaining the reasons of the study and what steps will be followed in order to achieve the goals.

Chapter 2 contains a detailed literature review about waste heat recovery technics developed until today, why the ORC is preferred in automotive Waste Heat Recovery (WHR), presents the best suitable working fluids, usage and characteristics, components used in a basic ORC, and finally presents a review on the expanders for such an application, as well as their main advantages and disadvantages.

Chapter 3 presents a methodology and calculations on how to select an expander for an automotive application, considering the common power that can be obtained through the vehicle's exhaust gas in the evaporator. A methodology will be determined and explained, and the NsDs chart will be used in order to find the most suitable expander for the points studied.

Chapter 4 shows the softwares available and used by previous authors. More importance will be given to the LMSImagineAMESim, which is the main subject of this work, and thermodynamic databases used for fluid conditions will also be described. It also describes the model developed in AMESim, all the components used and their description. Model validation is contained in the end of this chapter, but for confidentiality reasons, only points from chapter 3 will be used to explain which results can be obtain and how, and how to extract the results to graphics.

Chapter 5 contains de conclusions to this work and also the future studies that can follow.

2. Literature Review

2.1. Introduction

This chapter provides an explanation of the Rankine cycle system for automotive vehicle WHR applications, working fluids and components. Several articles are reviewed and commented, in order to compare the solutions studied and find the most promising combinations.

2.2. Waste Heat Recovery

It is well known that, in the Internal Combustion Engine (ICE) the greatest part of the energy generated by fuel combustion is dissipated into the environment as heat. However, part of this waste heat can be re-used for many applications, like producing mechanical or electrical power, either in industry or small ICE applications, such as automotive vehicles, Bureau of Energy Efficiency (n.d.).

The automotive ICE, despite its technological advances over the years, converts just about 25% of the fuel energy into mechanical energy. Figure 2.1 reveals that approximately 40% of the total energy is lost through the exhaust gas in form of heat, and that energy could be recovered to produce electrical or mechanical power.

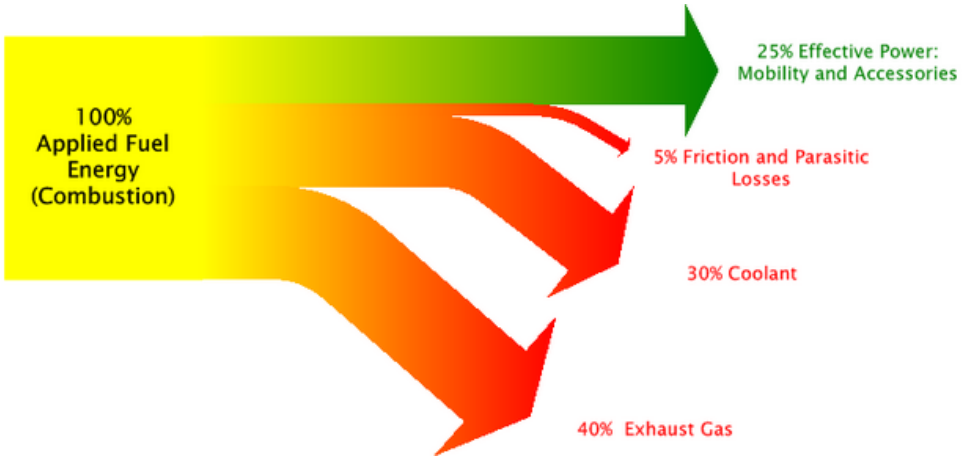

Figure 2.1 - Overall efficiency of an ICE, Sankey Diagrams (n.d.).

A great amount of studies have been carried worldwide on waste heat recovery technology to increase the efficiency of passenger cars and heavy duty vehicles. Rankine Cycle technology for automotive applications has been tested since 70's. For instance, Mack Trucks, Patel & Doyle (1976), designed and built a prototype of such a system operating on the exhaust gas of a 288 HD truck engine, and a 450 km on-road test demonstrated the technical feasibility of the system and its economic advantage with an improvement of 12.5% in fuel consumption. The space requirements and weight limitations for such a system are the biggest challenge for road vehicle applications.

The authors Freymann *et al.* (2008) also studied a system in which energy is recovered from both the exhaust gas and the cooling circuit. Endo *et al.* (2007) presented a system that recovered heat in the engine cylinder head, which means that the energy is also recovered from both sources. Oomori & Ogino (1993) studied a system that recovers heat only from the cooling circuit.

Regarding to the working fluids, the ORC showed to be the most suitable solution, thanks to a lower heat of vaporization of the organic fluids, that are preferable when the target power is limited and the temperature of the thermal source is low (100-220ºC), Wang *et al.* (2012), Cipollone *et al.* (2014). Due to the physical limitations, the expansion ratio, the minimum temperature difference between the hot and could source and the condensation temperature are important factors to be taken into account when studying this solution for automotive use, Macián *et al.* (2012).

Other similar ways to recover waste heat energy have also been studied, like the Brayton cycle, Song *et al.* (2013), the Turbo-generator Integrated Gas Energy Recovery System (TIGERS), Visteon UK (2005), the Electric Turbo-Compounding (ETC), Shoemaker (2014) and the Mechanical Turbo-Compounding (MTC), Kapoor (2013).

The Brayton cycle is an open gas power cycle with the working principle similar to the Rankine cycle, without the use of a condenser. The air intake takes place before the compressor and the exhaust happens after the expansion device, Song *et al.* (2013).

The Turbo-generator Integrated Gas Energy Recovery System (TIGERS) is a technology that uses a small turbo-generator to produce electrical power, instead of using it for turbocharging the engine. The small turbo-generator is installed just below the exhaust manifold in order to allow some of the high-energy exhaust gases to through it, which in turn drives the generator and creates electrical power. The system is claimed to create

powers up to 6 kW, which is enough to handle the vehicle's electrical systems. Other benefit is this system is more efficient than the normal belt-driven alternator because it is not affected by the parasitic losses from the mechanical support systems – reducing fuel consumption between 5% to 10%, Visteon UK (2005).

The Electric Turbo-Compounding (ETC) and Mechanical Turbo-Compounding (MTC) use a turbine to recover energy from the exhaust system and reintroduce it in the engine – in ETC, the energy is converted into electrical power and then transmitted to the engine by a power electronics module, and in MTC the energy is converted into kinetic energy and fed back into the engine via a high ratio transmission, Kapoor (2013).

In the Combined cycle, two engines are designed to work together to produce energy. The first engine burns fuel to create power and the exhaust gases are captured so that their heat is used in the second unit. The second unit is a Rankine system, in which the engine is the expansion machine, Tan (2005), Drescher & Brüggemann (2007), Quoilin & Lemort (2009).

2.3. The Rankine Cycle System

The Rankine Cycle (RC) is a closed thermodynamic cycle that allows the conversion of heat into mechanical work. The term ORC is applied to any RC that uses an organic fluid, most suitable for low grade heat source (80 to 300ºC), Woodland *et al.* (2012).

Figure 2.2a) and Figure 2.2b) show a schematic representation of a RC system and a T-s diagram of the ideal RC, respectively. As can be seen in the Figure 2.2a), the RC system uses a pump to raise de pressure of the fluid towards the heat exchanger. In the heat exchanger, the fluid raises its temperature using an external heat source (*e.g.* exhaust gases) and changes its phase from liquid to superheated vapor, and then flows through an expander machine where its high enthalpy is used to produce mechanical work. After the expansion process, the fluid goes through a condenser in order to change again to the liquid phase, and then back to the pump to begin the cycle again. For an automotive application, the exhaust gases of the ICE are used as heat source in the heat exchanger, and in the condenser the cold source can be the ambient air (direct cooling) or a refrigeration circuit (indirect cooling).

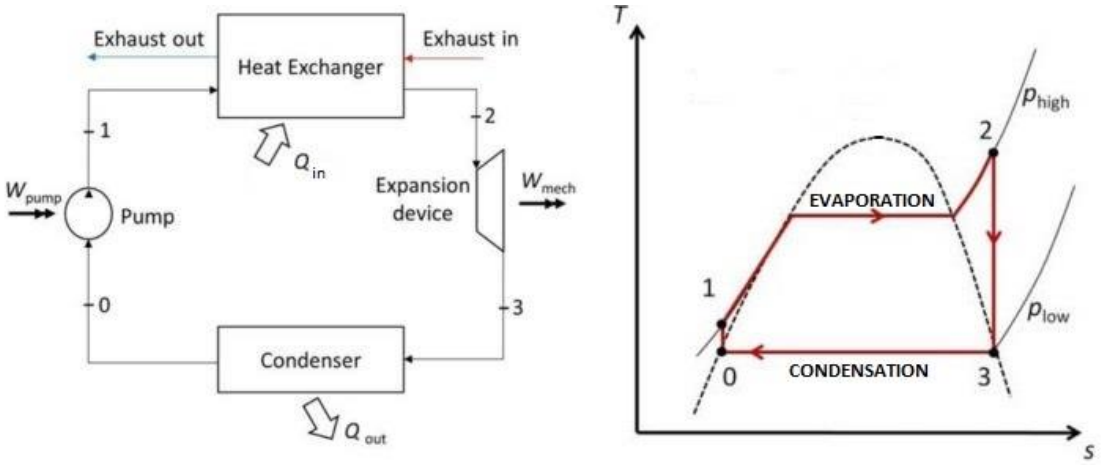

Figure 2.2 - a) Schematic representation of a RC system; b) T-s diagram of the ideal RC.

The Figure 2.2b) shows the ideal Rankine cycle in a T-s diagram. Before the pump, the fluid is in the lower temperature and entropy point (point 0). The pump raises the fluid pressure, from the condenser pressure to the heat exchanger pressure, while still in liquid state. Between the points 1 and 2, the fluid goes through the heat exchanger, changing its phase to superheated steam, and between 2 and 3 the fluid goes through the expander. Finally, the condenser reduces the energy of the fluid to its lowest entropy (points 3 to 0).

The thermal efficiency of the Rankine cycle is calculated through the ratio of the mechanical net power (difference between the mechanical work produced in the expander ($W_{mech,exp}$) and the pump work (W_{pump})), and the heat input in the heat exchanger (Q_{in}):

$$\eta_{th} = \frac{W_{mech,exp} - W_{pump}}{Q_{in}} \quad (1)$$

The amount of heat that can be recovered can be calculated as follows, Jadhao *et al.* (2013):

$$\dot{Q} = \dot{m} \times Cp \times \Delta T \quad (2)$$

In the equation 2, $\dot{Q}$ is the thermal power that can be recovered, $\dot{m}$ is the exhaust gas mass flow rate, Cp is the exhaust gas specific heat capacity and ΔT is the temperature gradient of the exhaust gas between the heat exchanger inlet and outlet. The higher the temperature at the heat exchanger inlet, the better is the quality of the heat, which indicates that the thermal efficiency of the RC (η_{th}) will be higher, Jadhao *et al.* (2013). Regarding to the heat exchanger, the value of the exhaust gas temperature profile must comply with

the Pinch Point Temperature Difference (PPTD), which should be at least 10 ºC higher than the inlet working fluid saturation temperature in the heat exchanger, Santos *et al.* (2011). The PPTD is the difference between the exhaust gas temperature and the temperature at which the working fluid begins to vaporize, so it must be considered as the smallest temperature difference in the heat exchanger, as illustrated in the Figure 2.3.

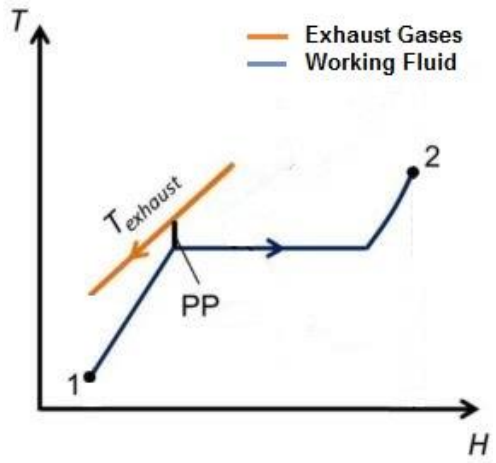

Figure 2.3 – T-H diagram illustrating the Pinch Point Temperature Difference (PPTD).

The overall cycle performance is significantly affected by the properties of the working fluid selected. The next section presents a detailed literature review on the working fluids that can be used in automotive RC applications.

2.4. Working Fluids

There are several studies on working fluids in order to determine which one suits best for a determined application. Variables like temperature and pressure have a large impact on the working fluid properties, and its saturation curves can be depicted in a T-s diagram. Figure 2.4 shows a representation of the saturation curves in a T-s diagram for different working fluids: a) isentropic; b) wet; c) dry.

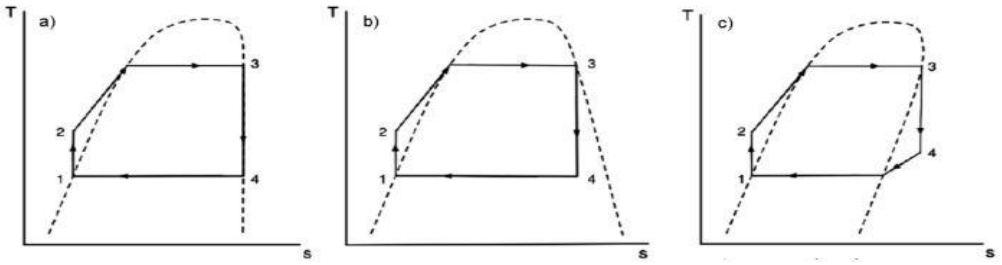

Figure 2.4 - T-s diagram for different working fluid types: a) isentropic; b) wet; c) dry, Santos *et al.* (2011).

Figure 2.4a) depicts that isentropic fluids have an almost vertical vapor saturation line (on the expansion side). Wet fluids have a negative slope vapor line and lead to droplets at the end of the expansion (see Figure 2.4b)), and as a result, they demand superheating before the expansion process in case of using a turbine, to guarantee that the expansion process ends outside the wet region. Dry fluids have a positive saturation curve and the expansion process ends in the superheated vapor region (see Figure 2.4c)), therefore a recuperator can be used in order to increase cycle efficiency, Santos *et al.* (2011), Quoilin *et al.* (2012), Latz *et al.* (2012), Latz *et al.* (2013).

Relatively to the thermodynamic characteristics, it is necessary to analyze the fluid's critical point, specific heat, density, etc., in order to determine its suitability. Regarding the environmental aspects, the values of the Ozone Depleting Potential (ODP) and the Global Warming Potential (GWP) must be low (particularly the ODP, which is being ruled out due to the Montreal Protocol, UNEP (1987)). In terms of side effects, flammability and toxicity must be considered (generally, engine exhaust gases reach about 500ºC, Hamilton & Hamilton (2015)) and the fluid must be the less toxic possible in case of system leakage.

For the working fluid selection, some criteria should be followed. Starting with the thermodynamic characteristics, then the environmental aspects and finally the side effects, it is necessary to fully check all these factors before selecting the appropriate fluid for the RC system, Quoilin *et al.* (2012). Thus, fluids with ODP should be excluded from the beginning because they will be ruled out in the future. The GWP may be considered of great importance too, but considering that the cycle is closed, this value may only be considered after a study of the fluids' Life-Cycle Assessment (LCA).

Some other considerations must be done for the appropriate selection of the correct working fluid. Organic fluids are more adequate than water for low heat sources due to lower heat of vaporization, Jadhao *et al.* (2013). The subcritical or supercritical Rankine

cycle has a large impact on the configuration of the physical system, for it may influence the amount of components required. For example, if a supercritical RC is employed it may be possible to achieve higher efficiencies without the need of an evaporator because the fluid is compressed to a pressure above its critical pressure, Latz *et al.* (2012). However, supercritical RC systems were disregarded from the present study due to safety issues.

The working fluids mostly considered for application in automotive vehicle WHR RC systems are showed in Table 2.1.

Table 2.1 - Properties of the working fluids that can be used for RC systems.

Working Fluid [source]	Ozone Depletion Potential ODP	Global Warming Potential GWP	Toxicity (Health Hazard (according to NFPA) H	Vapor Slope (Wet, Dry, Isentropic) W/D/I	Auto ignition Temperature [°C]	Freezing Point [°C]	Normal Boiling Point ($P_{atm} = 1\ bar$) [°C]	Critical Temperature T_c [°C]	Critical Pressure P_c [bar]	Density ρ [kg/m^3]
Water (Panesar *et al.* 2013) (Thorin 2000)	0	0	0	W	-	0	100	373.9	220.6	998.1
Ethanol (Panesar *et al.* 2013) (Clark 2005)	0	-	2	W	363	-114.1	78.5	240.9	61.4	791.9
R245fa (Panesar *et al.* 2013)	0	1030	2	D	412	-	15.3	154.1	36.4	1364.4
Water/Ethanol (azeotropic)	0	-	2	W	-	-	<78.2	-	191.9	-
Acetone (Panesar *et al.* 2013)	0	-	3	I	465	-94.7	56.3	235.1	47	784.9
R30 (Panesar *et al. 2013)*	<0.001	10	2	W	556	-95.1	39.8	236.9	60.8	1318.2
R1130 (Panesar *et al.* 2013)	0.00024	25	2	I	460	-49.8	47.7	243.4	55.1	1248.7
Methanol (Panesar *et al.* 2013) (Methanex 2006)	0	-	1	W	470	-97.6	64.6	239	78.5	794.4
Ammonia (Thorin 2000) (AirLiquid)	-	-	3	W	651	-77.7	-33.3	132.25	113.3	225
Toluene (ScienceLab) (Kavli Nanoscience Institute 2005)	-	-	2	D	480	-95	110.6	318.6	41	860
Ehyl-iodide (Panesar *et al.* 2013)	0	-	2	I	-	-111	47.1	280.9	47.1	1922.9
R-1234yf (DuPont 2014)	0	4	1	D	405	-150	-29.4	95.7	33.8	477.9
HCFC-123 (DuPont 2014)	0.02	93	1	D	770	-107	27.6	183.68	36.6	1578
HFC-152a (Qiao 2000)	0	124	-	-	454	-	-24.7	113.5	45.2	2701.4

- Information not available

Fluids may be categorized by pure (for example, water and ethanol) and mixed (water-ethanol, R245fa, among others). Mixed fluids can be azeotropic or zeotropic. An azeotropic fluid is a mixture of two or more fluids with similar boiling points that work as a single fluid; while a zeotropic fluid has different boiling points in which boiling them may result in fluid separation. In these mixtures, the boiling point is lower than the boiling

point of either substance. In water-ethanol mixture, a mixture with a 95,6% of ethanol and 4,4% of water results in a boiling point of 78,2 ºC, which is 0,3ºC lower than ethanol's boiling point and 21,8ºC lower than the water's boiling point, Latz *et al.* (2012), Clark (2005), Imelda (2011).

Teng *et al.* (2011) developed a Rankine cycle for a 10.8 HD engine, to investigate the fuel economy benefit. Ethanol was chosen among four working fluids: ethanol, water, R245fa and 50-50 wt% water-ethanol mixture. Ethanol showed advantages among the studied fluids because of a condensation pressure higher than 1 bar and evaporation pressure around 4 bar. Figure 2.5 shows the T-s diagram for the four fluids considered.

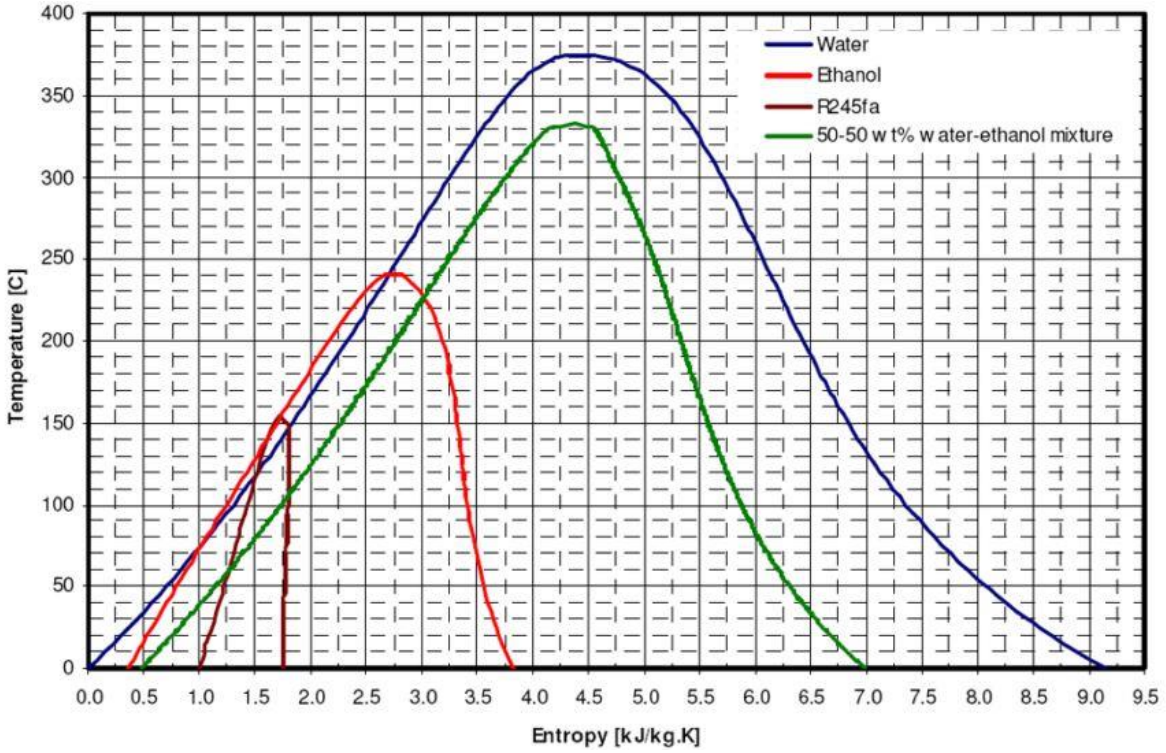

Figure 2.5 - T-s diagram of water, ethanol, R245fa and a water-ethanol mixture, adapted from Teng *et al.* (2011).

Latz (2013) also studied a system working on a water-ethanol mixture (containing 80% water and 20% ethanol), and found that this mixture is the optimal working fluid, offering a good trade-off between performance, safety, vehicle applicability, and lack of environmental issues. Organic fluids like refrigerants either performed poorly under the studied conditions or, aforementioned, had problems relating to high GWP and safety. In

this study, pure water was also excluded as a potential working fluid because it freezes at relatively high temperatures, as compared to the other working fluids (see Latz (2013)).

Haller *et al.* (2014) studied two Rankine cycle system arquitectures with two different expanders and four working fluids in total. In the low temperature (LT) RC system the fluids used were R134a and R245fa, and the expander selected was a scroll machine adapted from an air-conditioning system. Water and ethanol were used for the high temperature (HT) RC system, with a piston machine as expander. It was concluded that at an ambient temperature of 22°C, R134a or R245fa systems are more powerful than ethanol system for car velocity respectively less than 120 km/h and 135 km/h.

Panesar *et al.* (2013a) investigated the application of a RC system as a Bottoming Cycle (BC) applied in a 10 litre HDD engine for potential improvements in fuel efficiency. The authors reviewed a fluid selection methodology using seven working fluids: water, ethanol, R245fa, ethyl-iodide, R1130, R30 and acetone. Authors stated that the molecular weight of the working fluid has impact on the power required by the pump - fluids with less molecular weight require less pump power. Also, a fluid with lower Volume Flow Ratio (VFR) will result in a more compact expansion machine, reducing the system size. It was concluded that ethanol was the best solution but R1130, acetone and R30 were also good alternatives.

Seher *et al.* (2012) tested a RC system in a 12 L HDD and analyzed, by one dimensional simulation, two expansion machines - turbine and piston - and five working fluids: water, ethanol, HMDSO (hexamethyldisiloxane), R245fa and toluene. The boundary conditions at the inlet of the expander were 32 bar of maximum pressure and 380ºC of maximum temperature. The condensation temperatures were set to 100 ºC. For the turbine expander, all the five fluids were considered, and for the piston, only ethanol and water. Toluene showed to be the most favorable, but for being classified as harmful for health, it was not recommended. The organic fluid R245fa showed the lowest performance on the tested conditions. The work reveals that the best working fluids are ethanol and water with the piston expander and ethanol with the turbine expander.

Kunte *et al.* (2013) performed a study on a turbine expander, selecting ethanol instead of water, isopentane, R245fa and methanol, and limited the cycle to a maximum temperature of 276,85ºC to avoid ethanol decomposition. The minimum and maximum operating temperature of the turbine were established to be 70ºC and 256,85 ºC,

respectively, with a maximum pressure of 39,8 bar, ensuring a safe operation of the turbine. Ethanol was selected because it not only showed good behavior in power output, but also for its high molecular mass. Ethanol has a higher molecular mass than water and methanol, leading to a lower speed of sound and lower rotational speed of the turbine, for the same turbine diameter.

Galindo *et al.* (2015) presents an experimental study on a system that uses ethanol, in order to test a swash-plate piston expander. The authors claim that ethanol is one of the best solutions to recover thermal energy in a range of temperatures of 100ºC to 450ºC. Ethanol is environmental friendly, has high expansion ratios, condensation temperature at atmospheric pressure, low freezing point and is relatively cheap, with the only downside being the fact that it is highly flammable.

In resume, the extensive literature survey revealed that the ethanol and water-ethanol mixtures are the best candidates as working fluids for automotive vehicle RC systems. Water-ethanol has a good trade-off between performance, safety, vehicle applicability and lack of environmental issues, and ethanol shows good condensation and evaporation pressure and has a high molecular weight, which allows lower rotational speed of the turbine.

2.5. WHR System Components

The rankine cycle system is based in four main components: the pump, heat exchanger, expander and condenser. The pump raises the pressure of the fluid to a higher pressure level; the heat exchanger uses the heat from the hot exhaust gases to evaporate the working fluid, which is expanded in the expansion machine, producing power. The final step is returning the gaseous fluid into its liquid state, in the condenser.

In automobiles, the system must be compact and light, and for that reason, a single component has to do all the work for each step. However, some systems may have other additional components, like subcoolers or safety tanks. The subcooler is usually connected after the condenser and before the pump, and is used to avoid cavitation. As for the safety tank, a working fluid reservoir between the condenser and the pump may be used, preventing the uncondensed vapor from entering the pump.

2.5.1. Pump

The pump raises the pressure of the working fluid, between the condenser and the evaporator. When the compression happens, the fluid is in its liquid state, and with the fluid in liquid state, pumps can achieve very high efficiencies with high pressure ratios. For this reason, it has a small impact on the overall performance of the RC system, Lopes *et al.* (2012). Many pumps can be found in the market for many applications and different pressure ratios and fluids for being a widely used and developed technology. The pump speed shall be variable in order to meet the requirements for working fluid flows at the different load points.

Teng *et al.* (2011) used a Vickers VMW double-action 10 cc/rev vane pump, for its double action feature of this pump minimizes the internal leakage and friction. Besides, it is a rotary pump without the need of a separate lubrication system and handles cavitation better than a centrifugal pump.

Tahir *et al.* (2010) used a Rietschle Thomas 5002F Diaphragm mounted in a low temperature heat source system running on R245fa. It was displacing 0,140 l/m at a constant rate, and raising the fluid to a maximum of 2,9 bar at 80ºC. It was concluded that the pump power consumption was higher than expected (5 kW), lowering the overall thermal efficiency at around 19%.

Galindo *et al.* (2015) used a stainless steel plunger pump with direct drive from Cat Pumps, driven by an electric motor at a maximum of 1725 rpm and a volume flow rate of 7 l/min. The fluid used in the system was ethanol, and the maximum pressure achieved was 24,8 bar. The electrical power consumed by the pump was only 1% of the overall power balance of the system.

2.5.2. Heat Exchanger

The evaporator heat exchanger, also referred as boiler, is the component where the working fluid changes its phase from liquid to superheated vapor. Generally, it is a single part and includes the pre-heater, evaporator and superheater.

The biggest issue of the boiler heat exchanger in automotive use is its size and weight. It must be compact and light enough and still have good heat transfer

characteristics. Endo *et al.* (2007) developed an evaporator prototype integrated in the cylinder head, mounted externally to minimize modifications to the engine. Thus, densely layered multi-plate fins were adopted as heat transfer plates, and integrating the unit in the cylinder head reduces heat loss and size.

According to Lopes *et al.* (2012), evaporators can be divided in two main categories: tubes or plates (see Figure 2.6). Tube evaporators include the use of tubes to conduct and separate the working fluid from the hot source, in a wide variety of types, configurations and aspects. As for the plate evaporators, they are configured layers that create several levels of intermittent cold and hot source passages. Their design has to take into account the thermal source characteristics: type (liquid, gas, and vapour), relative temperature, mass flow, density and flow direction. In this study, the volume and cost were taken into account. Generally, for automotive use, weight may also be considered.

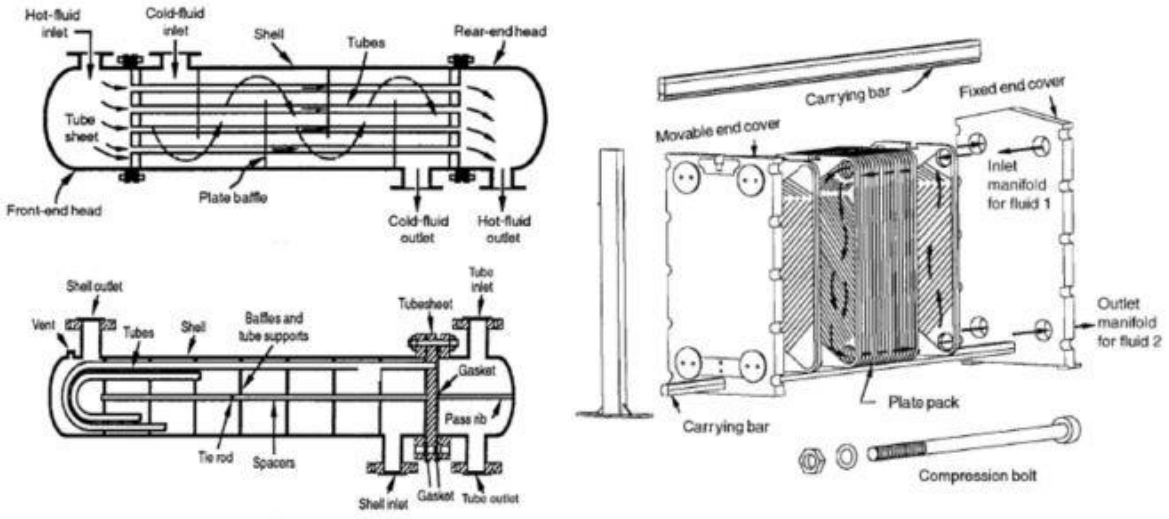

Figure 2.6 - Heat exchanger types: left – shell and tube; right – plate and fin, Lopes *et al.* (2012).

2.5.3. Condenser

The condenser works on the same principle as the boiler/heat exchanger, except that the working fluid is the hot source, and an external source will be the cold source – ambience air or a refrigeration circuit running on water or other fluid.

If air is used as the cold source, the cycle behavior may change if the vehicle is running in summer or cold winter temperatures, as the temperature difference between cold and hot sources is lower and the energy to be extracted is lower, Tahir *et al.* (2010).

If the expansion ends in the superheated vapor zone, condensation gets complicated and a large condenser may be required, Panesar *et al.* (2013b).

2.5.4. Expander

The expander is the component where the work output of the cycle is generated. Two main types of expanders can be distinguished: the dynamic (turbo) and displacement (volumetric) type, Santos *et al.* (2011). The working fluid goes in the expander at high pressure and temperature and is exhausted at low pressure and low temperature, which means a drop in the specific enthalpy of the working fluid inside the expander. The enthalpy drop is what the expander converts into work, Panesar *et al.* (2013b).

The performance of the expander strongly affects the performance of the RC system. There are many important parameters when selecting an expander such as the isentropic efficiency, pressure ratio ($PR = P_{inlet}/P_{outlet}$) or expansion ratio ($ER = V_{outlet}/V_{inlet}$), power output, lubrication requirements, complexity, rotational speed, dynamic balance, reliability, and cost. The fluid mass flow rate is also an important parameter for expander design and will significantly affect its efficiency.

The pressure ratio is the ratio between the pressure at the inlet and at the outlet of the expander (see equation 3), and it is a reference value for its optimal working conditions. The importance of this value lies on the fact that a machine is designed for a set of target operating conditions, which may vary a lot in an automotive RC application, and due to that the efficiency decreases when the system is running out of the off-design conditions. Kim *et al.* (2012) studied the optimization of the designed pressure ratio of two positive displacement expanders, by varying the vehicle operating conditions, in order to operate in both under and over-expansion states, concluding that the expansion efficiency decreased gradually during under-expansion operation, and rapidly during over-expansion operation. Under-expansion operation means that the design pressure ratio is lower than the operating pressure ratio, and over-expansion operation is the opposite (see Figure 2.7).

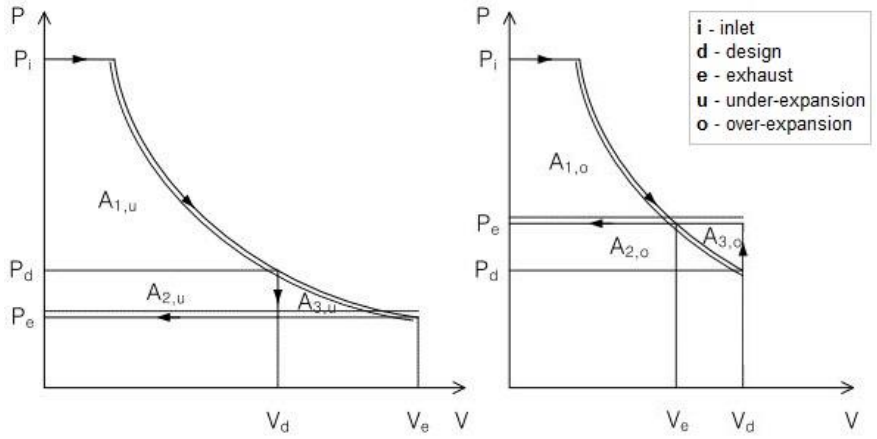

Figure 2.7 – Isentropic expansion in PV diagrams: a) under-expansion and b) over-expansion, Kim *et al.* (2012).

The isentropic efficiency of an expander is the ratio of the real power output achieved compared with the theoretical one, and can be calculated as follows:

$$\eta_s = \frac{Real\ work}{Isentropic\ Work} = \frac{h_3 - h_4}{h_3 - h_{4_s}} \tag{3}$$

The isentropic efficiency (η_s) is of major importance for the expansion process and strongly influences the overall RC system efficiency. Figure 2.8 depicts the expansion process for both real and isentropic cases: the process 3 to 4s corresponds to an isentropic expansion, and the process 3 to 4 corresponds to the real process. Point 4 is defined by the isentropic efficiency of the expander.

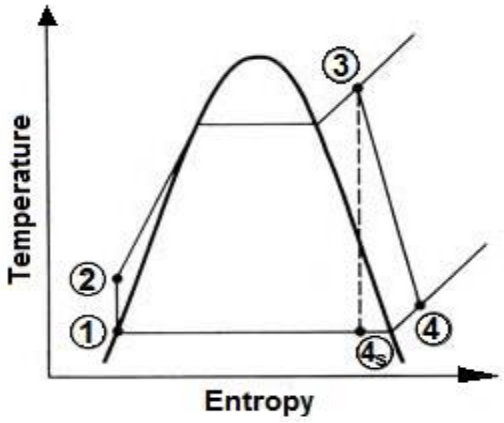

Figure 2.8 - Rankine cycle considering both isentropic expansion and real expansion, Stine & Geyer (2001).

The next section presents a literature review and a detailed explanation on the different expander types.

2.6. Expander Types

The expanders are classified in two main categories: the displacement type (volumetric) and the dynamic type (turbo), as can be seen in figure Figure 2.9.

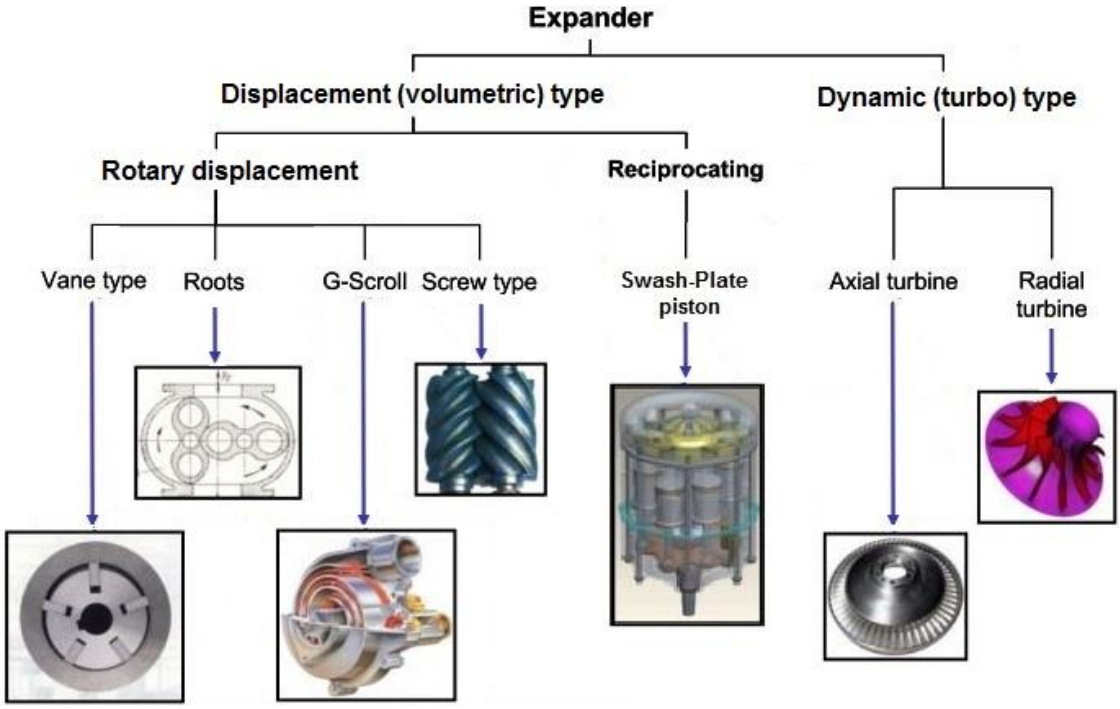

Figure 2.9 - Diagram of the various expander types, adapted from Dingel & Ambrosius (2014).

Displacement type machines are more appropriate for small-scale ORC units, because they are characterized by lower flow rates, higher pressure ratios and much lower rotational speeds than turbo-machines. Moreover, these machines can tolerate two-phase conditions, which may appear at the end of the expansion in some operating conditions, Lemort *et al.* (2009). The slow rotational speed of the displacement type expanders makes them good candidates for direct connection to the engine's shaft. However, they are heavier and bulkier than a turbine for the similar conditions, Latz *et al.* (2013).

On the other hand, turbine expanders achieve much higher rotating speeds than reciprocating expanders, making them very good in producing electrical power, where the expander is connected to a generator. There is also the possibility of connecting them to the engine's crankshaft, using a gearbox, Santos *et al.* (2011). However, turbine expanders are very sensitive to droplets, so they should only be selected in case of dry or isentropic

working fluids. If the working fluid is wet (e.g., water), reciprocating expanders are the most suitable.

Lopes *et al.* (2012) gathered the results of many studies for each different expander technology. Table 2.2 shows the values from the previous studies.

Table 2.2 – Values from previous studies found in Lopes *et al.* (2012).

Type	ε_i[%]	P_0[bar]	pr	T_0 [C]	$\dot{W}_{exp}$ [kW]	N[rpm]	Fluid	ε_{cycle}[%]	Year
Turbine	79	7.3	4.1	85	32.70	20,000	R245fa	6.1	2011
Turbine	85	2.2[a]	1.1	70	-	60,000	HFE-301	7.6	2006
Turbine	40	2.7[a]	1.1	95	-	60,000	n-Pentane	5.0	2006
Turbine	46[a]	3.4[a]	2.0[a]	70[a]	0.15[a]	35,000	R123	-	2001
Turbine	70[b]	25.0	25.0	220	6.03	4,000	Water	13.3	2005
Turbine	54[b]	22.5	8.0	143	6.66	4,000	R245fa	8.7	2005
Turbine	38[b]	19.0	8.0	151	6.63	4,000	i-Pentane	9.0	2005
Piston	62	7.8	2.4	-	-	306[a]	CO2	-	2006
Piston (Swash Plate)	-	80.0	-	500	2.98[b]	1,500[a]	Water	13.0	2007
Rotary Vane	48	-	-	90[b]	0.03	2,095[a]	R245fa	3.8	2010
Rotary Vane	23	90.0	1.4	44	-	800	CO2	-	2009
Rotary Vane	81	6.3	-	170	0.82	-	R123	-	2011
Rotary Vane	84	7.0	-	170	1.93	6,500	R123	-	2011
Gerotor	66	4.1	3.0[b]	84	0.67[b]	3,670	R123	-	2009
Gerotor	66	18.8	8.3[b]	146	2.67[b]	3,670	R123	-	2009
Gerotor	59	7.2	3.0[b]	130	1.38[b]	3,670	R123	-	2009
Gerotor	85	12.3	4.2[b]	150	5.30[b]	3,670	R123	-	2009
Gerotor	58	11.2	3.4[b]	157	2.63[b]	3,670	R123	-	2009
Gerotor	45	10.9	5.3[b]	160	2.96[b]	3,670	R123	-	2009
Scroll	68	10.0	5.0	142	-	2.296	R123	-	2009
Scroll	65	9.4[b]	8.6[b]	136	0.35	2,800	R113	7.0	2009
Scroll	48	5.5	3.9	174	0.19	1,053	R123	6.8	2008
Scroll	46	6.1	3.9	173	0.22	1,223	R123	6.6	2008
Scroll	50	6.4	3.8	169	0.26	1,287	R123	7.2	2008
Scroll	87	-	4.0	-	1.00	3,600	R245fa	-	2010
Scroll	31	5.9	5.5	96	1.18	3,500	HFE-7000	3.1	2010
Scroll	67	13.5	8.8[b]	127	1.46[b]	3,670	R123	-	2009
Scroll	81	18.2	5.5[b]	149	2.12[b]	3,670	R123	-	2009
Scroll	83	11.9	3.0[b]	120	1.53[b]	3,670	R123	-	2009
Scroll	83	17.9	3.1[b]	155	2.40[b]	3,670	R123	-	2009
Scroll	72	12.7	5.6[b]	128	2.58[b]	3,670	R123	-	2009
Scroll	59	15.0	6.1[b]	137	2.65[b]	3,670	R123	-	2009
Scroll	50	20.4	8.2[b]	154	3.95[b]	3,670	R123	-	2009
Scroll	48[a]	3.3	-	70	0.21[a]	891[a]	R134a	4.7[a]	2009
Scroll	65	13.0	-	65	2.05	2,000	R134a	7.5[a]	2007
Scroll	33	13.0	11.4	145	11.00[a]	1400	Water	--	2007
Scroll	65	32.8	2.0[b]	120	1.70	4,500	R1234yf	6.4	2011
Scroll	80[a]	25.0	10.0	160	2.88	-	R245fa	5.8	2011
Scroll	76	12.0	7.2[a]	75	1.75	2,500	R245fa	8.6	2011
Scroll	52	-	-	-	1.05	-	R123	-	2011

Most of the studies found in Table 2.2 were gathered for low temperature cycles, which is not adequate for automotive. Seher *et al*. (2012) studied a system mounted in a 12L HDD engine, using a single-cylinder piston expander. The system data is depicted in Table 2.3.

Table 2.3 – Compilation of the data of the system found in Seher *et al.* (2012).

	Water	Ethanol	Unit
Max. temperature of working fluid at expander intake	>400	240	[ºC]
Pressure of working fluid at condenser	1	2,3	[bar]
Maximum pressure of working fluid	40		
Expander displacement	0,9		[L]
Expander Stroke	81		[mm]
Piston diameter	87		

Bosch (2012) provides data for the technical features for the WHR system, for the piston machine (also available in Seher *et al.* (2012)) and for the turbine expander machine. The features can be seen in Table 2.4.

Table 2.4 - Technical features of WHR system applied to a HDD engine, Bosch (2012).

System	**Type**	RC system	
	Thermal Input	100 – 300 [kW]	
	Fuel Savings	around 5%	
	Lifetime	1,6 Million km	
Expanders	**Type**	Piston Machine	Turbine with transmission
		Single cylinder double-acting	Constant pressure turbine
	Displacement	0,9 [L]	-
	Mass (total)	around 40 kg	around 25 kg
	Max Power	25 [kW]	
	Max Temperature	300 [ºC]	
	Max. Pressure	50 [bar]	
	Power Take-off	Crankshaft via clutch, gear drive	Crankshaft via transmission and clutch, gear drive or generator

Latz (2013) performed a dimensionless analysis in two classes of expansion devices: displacement expanders and turbine expanders. The author uses the volume flow rate and the isentropic enthalpy drop of the working fluid over the expander as input variables. It was concluded that displacement expanders offered the highest thermal efficiencies when using a high expansion pressure ratio with a water-alcohol mixture as the working fluid. However, acceptable efficiencies could be achieved with single-stage turbine expanders by reducing the expansion pressure ratio and using an organic working fluid, both of which would increase the mass flow rate through the system.

From a thermodynamic point of view, the Rankine cycle is more efficient at high expansion pressure ratios. It would therefore be desirable to develop single-stage turbines that allow the use of high expansion ratios or compact multi-stage turbines, both of which would be easier to integrate into small vehicles compared to a more bulky displacement expander. However, in a previous study, Latz *et al.* (2013) states that multi-staged turbines increase their cost and complexity, which may be proved as an unsuccessful solution.

Table 2.5 presents a resume of the expander types investigated in previous studies.

Table 2.5 - Resume of the expander types investigated in previous studies.

Dynamic (turbo)	
Radial Turbine	(Seher et al. 2012)
Axial Turbine	(Seher et al. 2012) (Kunte et al. 2013) (Dingel & Ambrosius 2014)
Mixed Flow Turbine	(Seher et al. 2012)
Displacement (volumetric)	
Rotary Vane	(Lopes et al. 2012) (Tahir et al. 2010)
Scroll	(Lopes et al. 2012) (Lemort 2013) (Legros et al. 2014) (Lopes et al. 2012) (Lemort et al. 2009)
Screw	(Lemort 2013) (Legros et al. 2014)
Piston	(Seher et al. 2012) (Lopes et al. 2012) (Lemort 2013) (Legros et al. 2014) (Glavatskaya et al. 2012) (Berger 2014)
Swash-plate Piston	(Endo et al. 2007) (Lopes et al. 2012) (Kim et al. 2012)

2.6.1. Dynamic expanders (turbines)

Turbo-expanders operation is based on the high-pressure gas being directed past the turbine blades causing them to rotate as the gas expands. As stated before, turbines can be axial, radial or mixed flow, depending on the inlet flow direction. Figure 2.10 shows a cut-view of a turbine expander.

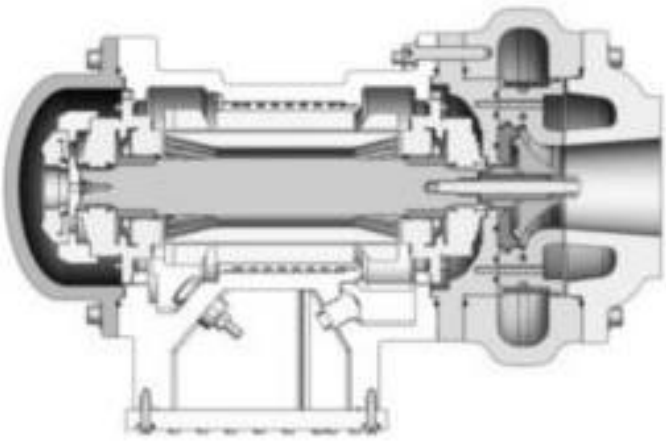

Figure 2.10 – Cut-view of a Turbine Expander, Lopes *et al.* (2012).

Turbine expanders operate at high rotating speeds (50000 rpm can be easily achieved, Panesar *et al.* (2013a), but can go up to 160000 rpm, Kunte *et al.* (2013), making them preferable to use in converting the energy to electricity.

Lopes *et al.* (2012) state that the most critical factor for high performance turbine expanders is be the blade speed ratio, given by the ratio between tip speed (*U*), and the isentropic spouting velocity (*C*), and that the optimal value for a radial turbine in a small-scale installation is 0,7 (velocity ratio, see eq. 4). Santos *et al.* (2011) state that the high speed of turbines is related to the blade Reynolds number (see eq. 5) and that this value should be on the order of 10^6, and also recommend a Mach number (see eq. 6) of 0,85 to avoid local choking on the flow rotor.

$$Velocity\ Ratio = \frac{U}{C} \tag{4}$$

$$Re_B = \frac{N \times D^2}{\nu} \quad (5)$$

$$Mach\ Number = \frac{U}{a} \quad (6)$$

In eq. 5, N is the rotary speed of the blade, D^2 is the diameter of the rotor and ν is the fluid's kinematic viscosity. In eq. 6, U is the velocity on the tip of the blade and a is the speed of sound.

As compared to other working fluids (like water) ethanol has a high molecular mass, leading to a lower speed of sound and as a result to a lower rotational speed of the turbine for the same turbine diameter.

According to Sauret & Rowlands (2011), that studied turbine expanders for geothermal applications, the author states that axial turbines handle higher flow rates than radial turbines, but radial turbines achieve higher pressure ratios. Also, from a mechanical point of view, radial inflow turbines are less sensitive to blade inaccuracies than axial turbines, maintaining high efficiencies as size decreases. They are also more robust under increased blade load using high density fluids, at both subcritical and supercritical conditions, and have higher stiffness, which improves rotor-dynamic stability of the system and makes them easier to manufacture because the blades are attached to the hub.

In resume, for small-scale applications, turbines must rotate at very high speeds in order to maintain optimal performance, single-stage turbines have low pressure ratios and they have shown to have isentropic efficiencies up to 85%. Also, if the expansion ratio is smaller than 50, they can achieve isentropic efficiencies higher than 0,8 with single stage only, Santos *et al.* (2011). They are precision machines that are expensive. The solution to round the low pressure ratio problem is to select multiple-stage turbines, which increases even more their cost.

2.6.2. Displacement expanders (volumetric)

The majority of the RC systems under research for automotive applications employ positive displacement machines, Lopes *et al.* (2012). Positive displacement expanders differ from the turbine expanders in the fact that they have a volume chamber, which limits the volume of the fluid inside the machine with each revolution.

2.6.2.1. Rotary vane expander

Rotary vane expander machines consist in a housing with inlet and exhaust, a rotor with vane slots and the vanes, and operate by the inlet of high temperature and pressure vapor that by expansion cause the rotor to move, which in turn increases the expansion volume. At the end of the expansion, the vapor is exhausted. Figure 2.11 shows the operation of the rotary vane expander.

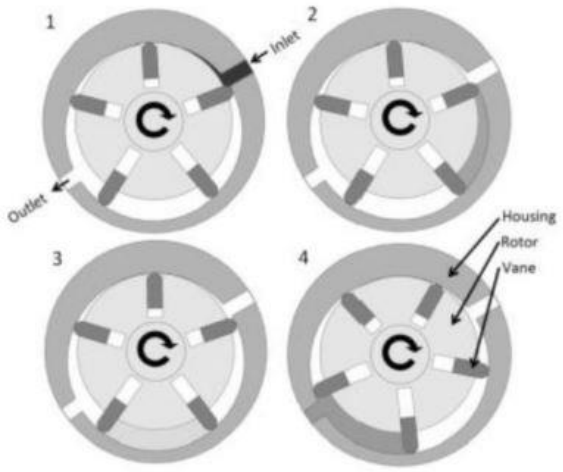

Figure 2.11 - Vane expanders operation. 1 – intake, 2 and 3 – expansion, 4 – exhaust, Lopes *et al.* (2012).

With the expansion process, the vanes are kept in contact with the housing by the means of springs or magnetic force, sealing the different volumes and isolating them. These type of expanders need lubrication and may suffer pressure drops of 65% and losses of 20% caused by leakages, due to the inability of the vanes to maintain a regular contact pressure against the housing, Lopes *et al.* (2012). Also, at higher speeds, frictional losses become more important, and high pressures may make the vanes bounce and strike against

the cylinder wall, reducing expander's life and performance, Lopes *et al.* (2012). They are tolerant to wet expansion and have a simple mechanism and minimal mechanical parts, which makes them very cheap, Santos *et al.* (2011).

2.6.2.2. Scroll expander

Scroll machines can be found in a large scale in the market as compressor machines. Besides, scroll air compressors may easily be adapted to work as expansion machines for testing purposes. It only has one moving part and consists in two spirals, one moving in eccentric circles and one stationary. The fluid goes in through an orifice in the center of the spiral and gets transported to the side, expanding on the way and consequently rotating the spirals.

Scroll expanders can be categorized in two types: compliant and constrained, Lopes *et al.* (2012). A compliant scroll requires lubrication and uses the centrifugal effect to keep the orbiting scroll in continuous contact with the fixed scroll, and a constrained scroll can operate without lubrication and be constrained either radially, axially or both. Their manufacturing tolerance must be considered as a critical parameter in case of a constrained type, having higher leakages and friction losses than a compliant type. The presence of oil inside the expander is a problem of big importance because it may mix with the working fluid inside the scroll, changing its properties. Also, there is the problem of radial leakages and friction losses, which cause poor performance, Lopes *et al.* (2012). The maximum internal built-in volume ratio is usually inferior to 5, Santos *et al.* (2011), Lemort (2013). The built-in volume ratio corresponds to the displacement volume of the expander machine. Figure 2.12 shows the two main leakage types in a scroll expander.

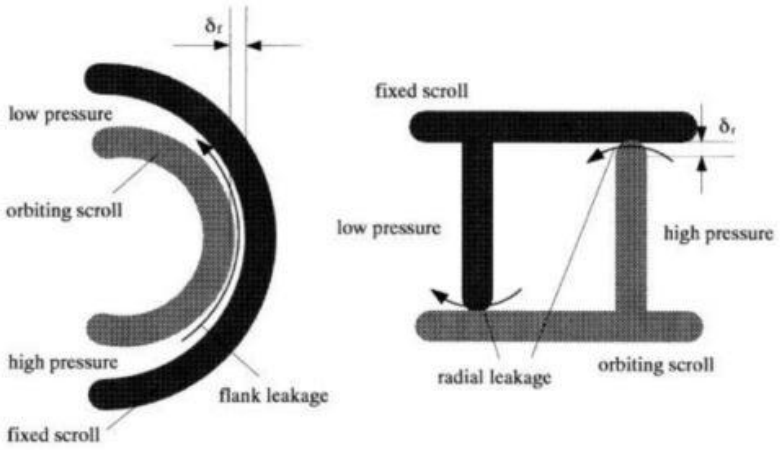

Figure 2.12 - Two main leakage types in a scroll expander, Lopes *et al.* (2012).

The displacement volume of scroll expanders usually varies between 1,1 l/s to 49 l/s and the rotational speed values can range between 1000 rpm and 4000 rpm (see Table 2.2). Built-in volume ratio is generally between 1,5 and 3,5, because higher values can cause sealing problems. The pressure ratio of scroll machines for expander operation may be up to 15, and selecting this type of expander for high discharge temperature applications is not recommended, the high temperature operation can cause degradation of the lubricant oil. Maximum operating temperatures of 165 and 215ºC for air and steam (respectively) were achieved in previous studies, Legros *et al.* (2014).

Kim *et al.* (2012) used a scroll expander with a displacement of 40 cm^3 and a rated driving speed of 3600 rpm in the study for the low temperature RC system (see Figure 2.13).

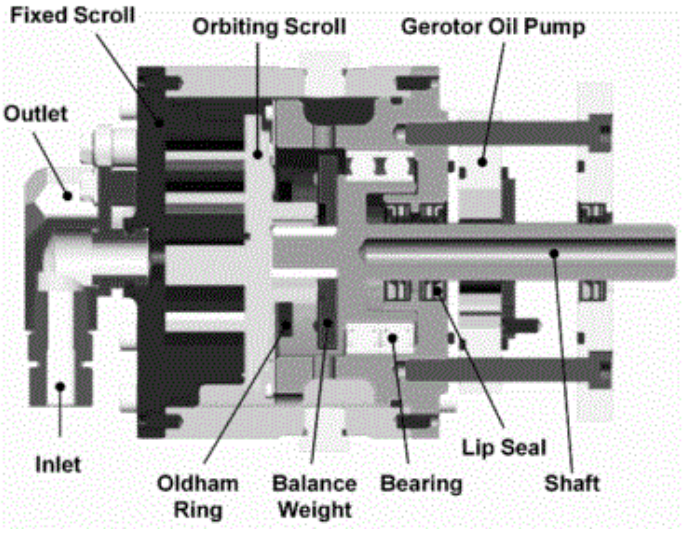

Figure 2.13 - Scroll expander used in the LT cycle by Kim *et al.* (2012).

2.6.2.3. Screw expander

Screw expanders operate by inletting the working fluid on the intake side, trapping the fluid between the blades and the housing as it moves forward, which expands and rotates the screws on the way to the exhaust side. The fluid is then expelled through the exhaust.

Figure 2.14 - Twin Screw Expander, Langson (2008).

The power range of screw machines is between 20 kWe and 1 MWe with displacement volumes going from 25 l/s to 1100 l/s. They can achieve high rotational speeds (up to 25000 rpm), can be synchronized or unsynchronized and require lubrication. The typical built-in volume ratio is around 5 and they can tolerate high temperatures (490ºC) and high pressure ratios (Nikolov *et al.* (2012) considered a value of 50 with ethanol). Screw type compressors are widely found in the market. For instance, they are commonly used in automobiles and heavy duty industrial machinery as superchargers. Small screw machines can compete with big scrolls, and their only moving parts are the screws. Screw type expanders can be found in geothermal systems running on steam, Lopes *et al.* (2012). The main drawback is the manufacturing precision required, especially in the synchronized ones.

This type of expander is a good solution for heavy industrial systems. Nevertheless, for automotive vehicles, screw expanders are turned down because of their size, weight and power.

2.6.2.4. Piston

Piston machines work according to the same principle as reciprocating ICEs, based in four main processes – intake, compression, power and exhaust (Figure 2.15).

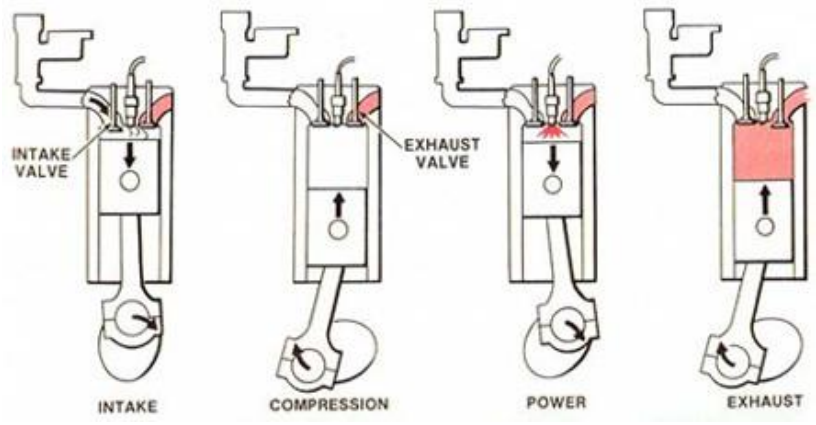

Figure 2.15 – Piston expander machine – working principle.

For ICEs four stroke engine, the intake process occurs while the piston is moving down inside the cylinder. When it starts moving back up, the intake valve closes the compression process occurs. Then, after reaching the top of the cylinder, the combustion occurs and the piston is forced down (power). Finally, after reaching the bottom, the exhaust valve opens and the resulting combustion gas exits the cylinder.

As expansion machines, the working principle is the same, but the inlet and expansion occur simultaneously, and the expansion is independent (Figure 2.16).

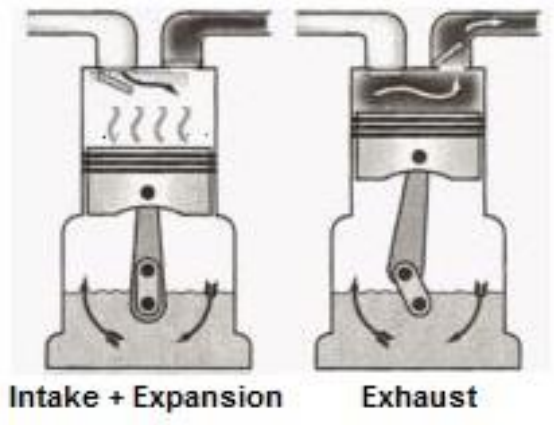

Figure 2.16 – Piston expander machine working principle, Lopes *et al.* (2012).

The first process (intake and expansion) occurs with the exhaust valve closed. The piston is at the top of the cylinder and the inlet valve opens, letting the high pressure and high temperature fluid enter de cylinder, and driving the piston down in the process. When the piston reaches the bottom, the inlet valve closes and the outlet valve opens, letting the working fluid (now with lower pressure and low temperature) exit the cylinder, while the piston moves upwards. After the piston reaches the top of the cylinder, the cycle begins again.

The inlet valve can be rotating, sliding or poppet, and for the exhaust, there can be either valves or ports, Lemort (2013). Figure 2.17 show both the real and ideal PV diagram and the valve lift diagram of a typical piston machine.

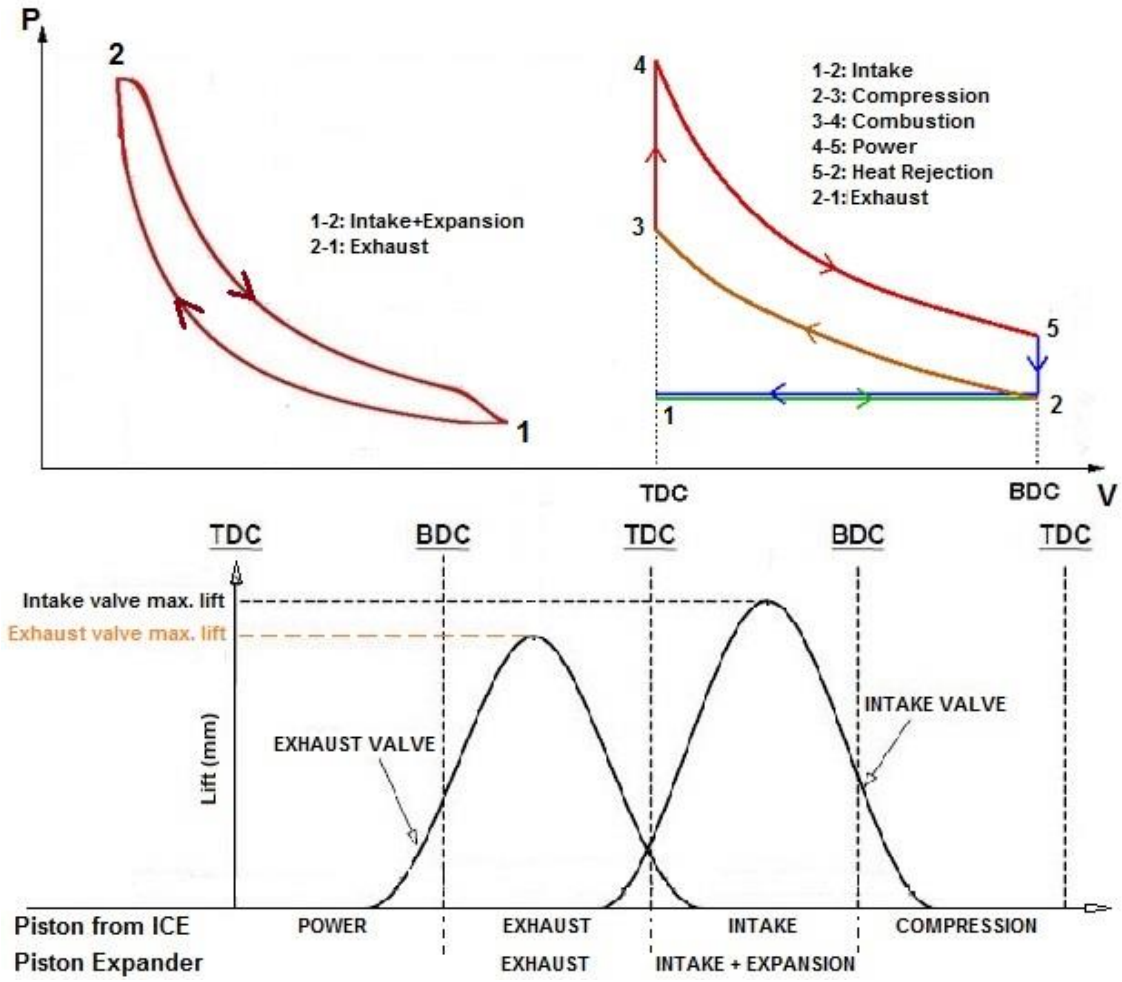

Figure 2.17 – Piston machine diagrams - Top Left: Real PV; Top Right: Ideal PV, Wikipedia (n.d.); Bottom: Valve Lift.

The reciprocating-type expander seems to be considered more appropriate for combining mechanical energy output directly to the crankshaft, in particular for on-road vehicle applications where the condition for waste heat is variable, because of its flexibility, Lopes *et al.* (2012). When compared to scroll and rotary vane expanders, they are preferred because they are suitable for higher pressure ratios, which allows a better efficiency of the global RC system, Galindo *et al.* (2015). They have high resistance to water droplets, tolerate high working fluid pressures and work well under large volume ratios. The drawbacks are the friction losses at higher pressures and possible sealing problems on the piston contact with the cylinder wall, Santos *et al.* (2011).

Built-in volume ratios between 6 and 14 are usually achieved for piston expanders, thus they tolerate large pressure ratios. The volume displacement of typical reciprocating-type expanders ranges from 1,25 l/s to 75 l/s, Lemort (2013). The rotational speed is similar to that achieved by ICE's. Temperatures can go up to 500ºC and pressure ratios relatively similar to ICE's, according to Legros *et al.* (2014). Piston expanders from EXOES (2011) achieve speeds between 500 and 6000 rpm.

2.6.2.5. Swash-plate piston expander

The present work considers a swash-plate expander type, which is also in the category of the piston expanders.

Galindo *et al.* (2015) claim that the swash-plate piston expanders are increasingly taking into account among the reciprocating type due to their versatility, compactness, robustness and good specific power.

Endo *et al.* (2007) studied a system in a swash-plate piston expander (see Figure 2.18), with 7 cylinders, a geometric expansion ratio of 14,7 and a maximum rotating speed of 3000 rpm. The expander allows a maximum temperature of 500ºC and pressure of 90 bar. The application of a RC system using a swash-plate piston expander allowed the thermal efficiency of the base vehicle to increase from 28,9% to 32,7%, which means a 13.2% relative increase.

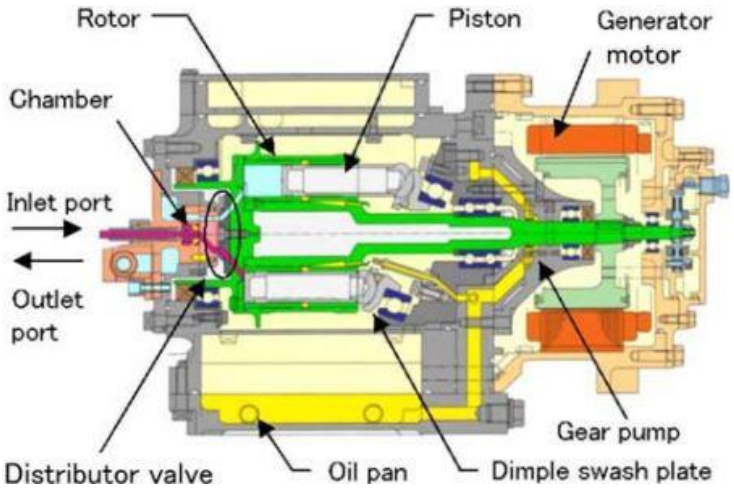

Figure 2.18 - Swash plate piston expander from Endo *et at.* (2007).

Kim *et al.* (2012) also used a swash-plate piston expander for their high temperature (HT) cycle. The expander had 5 cylinders, a piston diameter of 30 mm, a displacement of 108 cm^3, and a rated driving speed of 2450 rpm (see Figure 2.19).

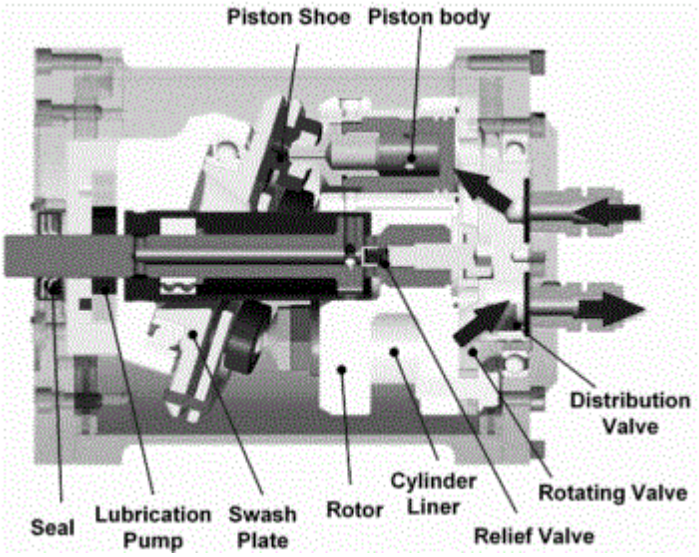

Figure 2.19 - Swash plate piston expander used by Kim *et al.* (2012).

3. Expander Selection

3.1. Introduction

The previous chapter provides a detailed review on the different types of expanders that can be used in RC systems for automotive application. This chapter is dedicated to the expander selection. To this end, the selection parameters and methodology applied for the expander selection are explained.

This chapter starts with the parameters used to select an expander machine and describes the NsDs turbine chart. A detailed explanation of the steps required to obtain the points in the chart will be given and a verification of the methodology using 3 different working fluids will then be performed.

3.2. Selection parameters

The waste heat provided by an automotive vehicle varies accordingly to the ICE's operating conditions, so a RC system designed to work under a certain target operating condition will sometimes operate under off-design conditions, and so that the pressure ratio is strongly affected with these constantly varying conditions. Kim *et al.* (2012) studied a dual loop system solution in order to avoid this problem, using a HT (high temperature) cycle with a swash plate piston expander and a LT (low-temperature) cycle with a scroll expander, covering both high and low heat sources and optimizing the overall working conditions of the cycle. It was concluded that for both cycles, with only a decrease in around 7% of the expansion efficiency, the weight and volume of the expanders would be decreased in approximately 39% for the HT cycle and 33% for the LT cycle.

The company Barber-Nichols proposed a NsDs chart that allows to select the optimal expander type as a function of the dimensionless parameters: specific speed (Ns) and specific diameter (Ds) for each use case. Figure 3.1 depicts the NsDs turbine chart. It is based on a similarity concept that states that the number of parameters describing the characteristics of an expansion machine can be reduced to four dimensionless numbers: i) the Mach number (Ma); ii) the Reynolds number (Re) at the inlet of the expander (which

have secondary effects on the expander's behavior); iii) the specific speed (N_S) and iv) the specific diameter (D_S), Keneth (1959), Latz *et al.* (2013), Sauret & Rowlands (2011). The eq. 7 and eq. 8 allow the calculation of the specific speed (N_S) and the specific diameter(D_S):

$$N_S = N_{exp} \times \frac{\sqrt{\dot{V}_{out}}}{\Delta H^{3/4}} \tag{7}$$

$$D_S = D_{exp} \times \frac{\Delta H^{1/4}}{\sqrt{\dot{V}_{out}}} \tag{8}$$

In the eq. 7, N_{exp} is the rotating speed [rpm] and $\dot{V}_{out}$ is the volumetric flow rate at the expander outlet [ft^3/s]. In the eq. 8, D_{exp} is the diameter [ft]. In both equations, ΔH is the specific enthalpy drop in height of fluid [ft].

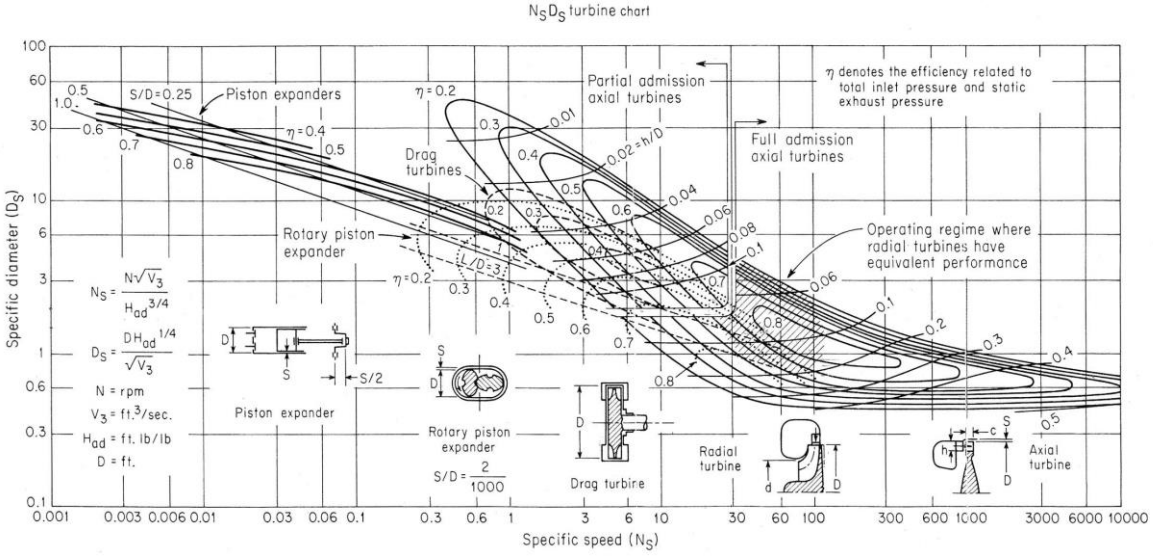

Figure 3.1 - Barber Nichols "how to select turbomachinery for your application", Keneth (1959).

In addition to the Barber Nichols turbine chart, the Figure 3.2 and Figure 3.3 show the Dixon's turbine chart and the Japikse's expander machine solution chart, respectively, Sauret & Rowlands (2011). The Dixon's turbine chart is used specifically for turbine type expanders and the Japikse's expander machine selection chart is for any expander type. Barber Nichols' chart uses imperial units and Dixon's chart uses metric units. The other input of the Dixon's chart is the overall efficiency of the turbine (η_t), as can be seen in Figure 3.2.

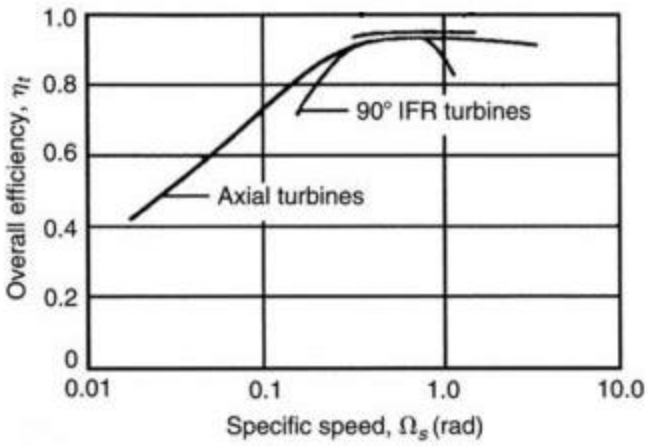

Figure 3.2 – Dixon's turbine chart (adapted from Dixon (1977)).

The specific speed (Ω_S) in Figure 3.2 is calculated through eq. 9:

$$\Omega_S = \frac{\Omega Q^{1/2}}{(gH)^{3/4}} \tag{9}$$

In eq. 9, Ω is the rotary speed [rad/s], Q is the volumetric flow rate $[\mathrm{m}^3/\mathrm{s}]$, g is the acceleration of gravity $[\mathrm{m}/\mathrm{s}^2]$ and H is the head of fluid [m].

For Japikse's chart, the inputs are the flow coefficient (ϕ), the head coefficient (Ψ) and the specific speed (N_S). The calculations required for the Japikse's chart are in metric units. The chart is presented in Figure 3.3.

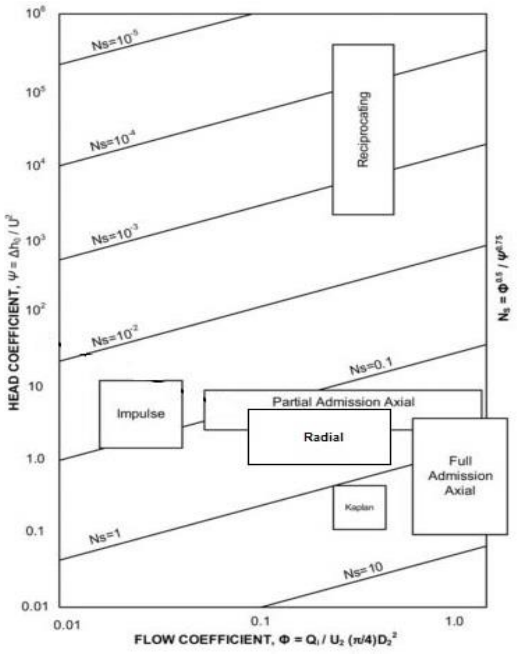

Figure 3.3 – Japikse's expander machine selection chart (adapted from Sauret & Rowlands (2011)).

Eq. 10, 11 and 12 are used as inputs in the graph of the Figure 3.3.

$$\phi = \frac{\mathrm{Q}_{in}}{U_2 \left(\frac{\pi}{4}\right) D^2} \tag{10}$$

$$\Psi = \frac{\Delta H}{U^2} \tag{11}$$

$$N_S = \frac{\phi^{0,5}}{\Psi^{0,75}} \tag{12}$$

In eq. 10, ϕ is the dimensionless flow coefficient, Q_{in} is the inlet volume flow rate $[\mathrm{m}^3/\mathrm{s}]$, U_2 is the speed at the outlet of the expander $[\mathrm{m}/\mathrm{s}]$ and D is the diameter of the expander [m] (in case it is a turbine, D is the diameter of the outlet rotor). Eq. 11 stands for the head coefficient (Ψ), where ΔH is the variation of the height of fluid [m] and U is the speed of the fluid at the inlet of the expander $[\mathrm{m}/\mathrm{s}]$. In eq. 12, N_S is expressed in $[\mathrm{m}/\mathrm{s}]$. The detailed explanation of the equations can be found in Dixon (1977).

The values obtained for each chart are different for the same type of machine. According to Sauret & Rowlands (2011), for radial-inflow-turbine expanders, the typical values for the specific speed should be: i) between 30 and 100 for the Barber Nichols's chart; ii) between 0,1 and 1 in the Japikse's chart and iii) 0,5 and 0,9 in the Dixon's chart.

For this work, the chart used for the machine selection is the Barber Nichols, in imperial units.

3.3. Methodology

The working fluid operating conditions at the expander inlet depends on the evaporator (boiler) operating conditions. Therefore, with the working fluid conditions at the inlet of the expander already determined by the working fluid conditions at inlet and outlet of the evaporator, as well as its thermal power, it is possible to determine the working fluid mass flow rate in the RC system, which is important to define the parameters required for the expander selection using the NsDs expander chart. Figure 3.4 shows a diagram of a step-by-step methodology for the determination of the points for the NsDs expander chart, and consequently the type of expander for a specific application.

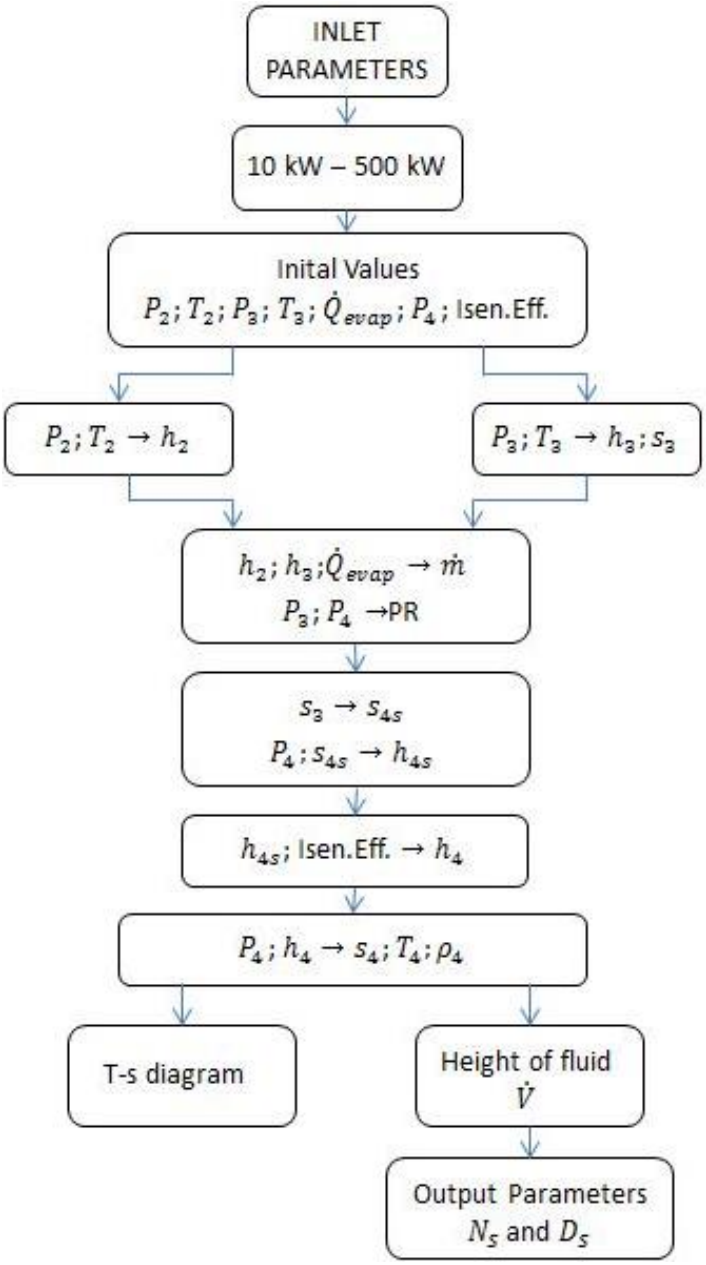

Figure 3.4 – Diagram that describes the sequence used to calculate de Ns and Ds parameters.

Initially, the pressure and temperature at the inlet of the evaporator (P_2;T_2) and at the evaporator outlet (P_3;T_3) are defined, and using the REFPROP, Lemmon *et al.* (2010), EES, FChart (n.d.), or other similar thermodynamic software, the enthalpies ($h_2; h_3$) and the entropy (s_3) are determined. Note that the state 3 corresponds to the inlet of the expander, considering that the ducts are short and will not have great influence in the theoretical calculations.

Another value given initially is the power of the evaporator ($\dot{Q}_{evap}$), and with the inlet and outlet enthalpies obtained in last step, the mass flow rate of the working fluid can be calculated using eq. 13. Also, having the pressure at the inlet of the expander (P_3) and the pressure at the outlet of the expander (P_4), the pressure ratio (Π) can then be calculated through eq. 14.

$$\dot{m} = \frac{\dot{Q}_{evap}}{h_3 - h_2} \tag{13}$$

$$\Pi = \frac{P_3}{P_4} \tag{14}$$

The step is determining the isentropic enthalpy at the expander outlet. For that, the isentropic entropy (s_{4s}) is needed. For the isentropic expander process the entropy at the outlet of the expander (s_{4s}) is equal to the entropy at the inlet (s_3). The isentropic enthalpy (h_{4s}) can then be calculated accordingly, using the pressure at the outlet of the expander (P_4) and the isentropic entropy (s_{4s}) as reference values.

Using the isentropic efficiency definition, the enthalpy at the outlet of the expander (h_4) can be calculated as follows:

$$h_4 = h_3 - \eta_s(h_3 - h_{4_s}) \tag{15}$$

After that, by using the pressure (P_4) and the enthalpy (h_4) at the outlet of the expander the state 4 is defined and as a result, the remaining thermodynamic properties (such as s_4, T_4 and ρ_4) can be obtained.

Next step is calculating both the height of fluid (ΔH) and the volume flow rate ($\dot{V}$), using equations 16 and 17, respectively.

$$\Delta H = \frac{h_4}{g} \tag{16}$$

$$\dot{V} = \frac{\dot{m}}{\rho_4} \tag{17}$$

In eq. 16, ΔH is the head of the fluid [m], h_4 is the enthalpy [J/kg] and g is the gravitational acceleration [m/s^2]. In eq. 17, $\dot{V}$ is the volumetric flow rate [m^3/s], $\dot{m}$ is the mass flow rate [kg/s] and ρ is the density of the fluid [kg/m^3].

To calculate the specific speed (N_S) and the specific diameter (D_S), the head of fluid (ΔH), the volumetric flow rate ($\dot{V}$) and the diameter (D) must be converted from SI units to Imperial units, using the conversions ($1\ ft = 0{,}3048\ m$; $1\,\frac{\mathrm{ft}^3}{\mathrm{s}} = 0{,}028316846\ \frac{\mathrm{m}^3}{\mathrm{s}}$).

3.4. Selection of an expander for an automotive RC system

For automotive vehicles RC system application, the evaporator works in a power range between 10 kW and 500 kW. The corresponding working fluid mass flow rate is calculated through eq. 11. To that, for each working fluid evaluated (R245fa, ethanol and water), a minimum and a maximum mass flow rate will be calculated. From this will result a region in the NsDs expander chart limited by the two corresponding NsDs points obtained, one minimum and one maximum.

Such as already referred three fluids were used for the present study analysis: R245fa, ethanol and water. Ethanol and R245fa were selected because of the potential showed in previous studies for small-scale RC applications, Panesar *et al.* (2013b), Wang *et al.* (2011), and water was selected for comparative reasons for it is a non-flammable and non-toxic fluid and is used for many energy recovery systems, Lopes *et al.* (2012), Panesar *et al.* (2013b).

Figure 3.1 shows a diagram with the working fluid properties used to start the calculations, according to the point in the system and the working fluid in use.

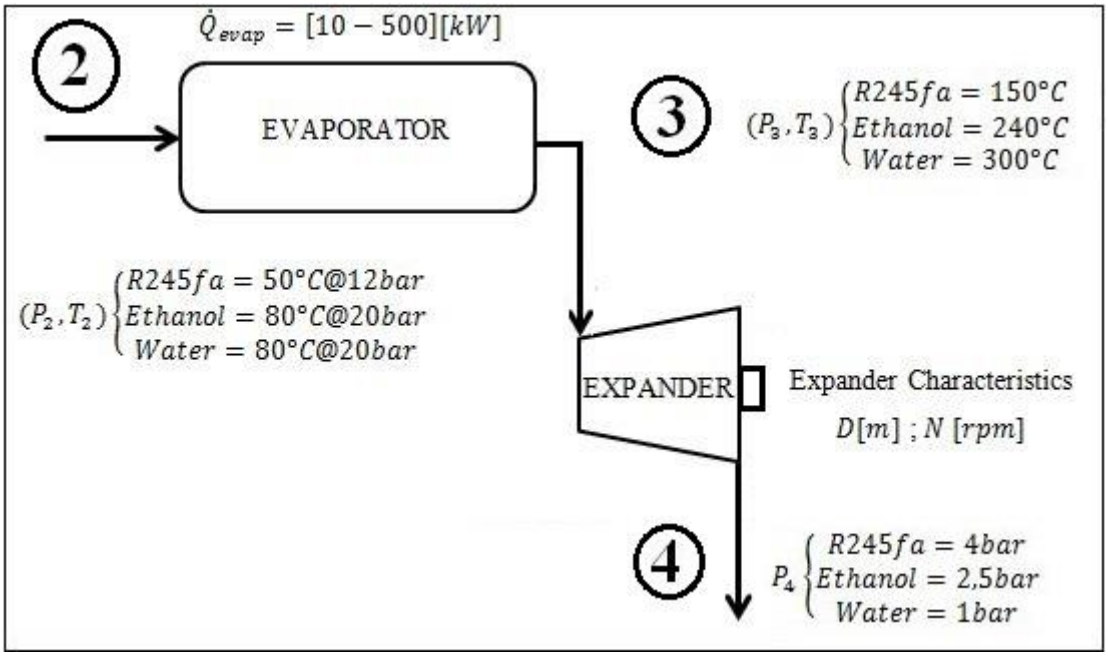

Figure 3.5 – Diagram of the process and initial values for calculations.

The pressure at the inlet and outlet of the evaporator are equal (isobaric process), so it will be named as evaporation pressure (P_{evap}), and the pressure at point 4 will be named as condensation pressure (P_{cond}). Table 3.1 resumes the properties for each working fluid.

Table 3.1 – Resume of the thermodynamic properties.

	T_2 [°C]	T_3 [°C]	P_{evap} [bar]	T_{evap} [°C]	P_{cond} [bar]	T_{cond} [°C]
R245fa	50	150	12	97,657	4	54,995
Ethanol	80	240	20	180,42	2,5	103,08
Water	80	300	20	212,38	1	99,6

Speed and diameter of the expander were selected according to previous studies, for both displacement and turbine expander machines, Lopes *et al.* (2012), Galindo *et al.* (2015), Declaye *et al.* (2013). For the diameter and rotational speed of the expanders, the literature review demonstrated that a value of 0,03 [m] for the diameter was appropriate for the calculations, and that for the rotational speeds, more values should be tested in order to cover the range studied in previous works, Kunte *et al.* (2013), Kim *et al.* (2012), Lemort

et al. (2009), Lopes *et al.* (2012), Endo *et al.* (2007). Six different test conditions will be performed for the three different working fluids (see Table 3.2). Considering the test conditions in the Table 3.2, the test conditions 1, 2 and 3 represent rotational speeds that are suitable for displacement expanders (1000 rpm to 3000 rpm), and the test conditions 4, 5 and 6 correspond to rotational speeds suitable for turbine expanders (20000 rpm to 10000 rpm).

Table 3.2 – Rotary speeds used for calculations.

	Test Condition	Speed [rpm]	Diameter [m]
Displacement Expanders	1	1000	0,03
	2	3000	
	3	5000	
Turbine Expanders	4	20000	0,03
	5	50000	
	6	100000	

Table 3.3 presents a resume of the input parameters used in the calculations. Two mass flow rates were calculated according to the minimum and maximum limits chosen for the evaporator (10 kW and 500 kW) for automotive applications. The higher the evaporator power, the higher the mass flow rate obtained.

Table 3.3 – Excel table with the thermodynamic inputs.

	R245fa				Ethanol				Water			
P_2	12,00	bar	1,20	MPa	20,00	bar	2,00	MPa	20,00	bar	2,00	MPa
T_2	50,00	°C	323,15	K	80,00	°C	353,15	K	80,00	°C	353,15	K
h_2	210,37	kJ/kg			336,57	kJ/kg			336,57	kJ/kg		
P_3	12,00	bar	1,20	MPa	20,00	bar	2,00	MPa	20,00	bar	2,00	MPa
T_3	150,00	°C	423,15	K	240,00	°C	513,15	K	300,00	°C	573,15	K
h_3	536,86	kJ/kg			1543,77	kJ/kg			3024,18	kJ/kg		
	$\dot{m}_{min}$	$\dot{m}_{max}$			$\dot{m}_{min}$	$\dot{m}_{max}$			$\dot{m}_{min}$	$\dot{m}_{max}$		
$\dot{m}$	0,031	1,53	kg/s		0,008	0,414	kg/s		0,004	0,186	kg/s	
	30,63	1531,4	g/s		8,28	414,18	g/s		3,72	186,04	g/s	
PR	3,00				8,00				20,00			
P_4	4,00	bar	0,40	MPa	2,50	bar	0,25	MPa	1,00	bar	0,10	MPa

Considering the evaporator thermal power in the range 10 kW to 500 kW and the working fluid operating conditions (see Table 3.1), the working fluid mass flow rate ranges from: i) 30,63 g/s to 1531,4 g/s for R245fa; ii) 8,28 g/s to 414,18 g/s for ethanol and iii) 3,72 g/s to 186,04 g/s for water. Considering the evaporator and condenser pressures, the pressure ratio (PR) is: 3 for R245fa, 8 for ethanol and 20 for water.

Table 3.4 shows the input values for the expander and also the resultant specific speed (N_S) and specific diameter (D_S). The minimum value of each fluid corresponds to the minimum (10 kW), and the maximum (500 kW) evaporator power.

Table 3.4 – Excel table with the values for the expander and the resultant specific speed and specific diameter (test condition 1, see Table 3.2).

							NsDs chart Bajle					
Point	Name	Fluid	mass flow	speed	Diameter		Height		Vol flow		S.Speed	S.Diameter
			ṁ	N	D		ΔH		V		Ns	Ds
			[kg/s]	[rpm]	[m]	[ft]	[m]	[ft]	[m3/s]	[ft3/s]	[-]	[-]
1a	min_R245fa	R245fa	0,031	1000	0,16	0,525	52967	173776	0,0018	0,0636	0,030	42,49
1b	max_R245fa		1,531						0,090	3,181	0,210	6,01
2a	min_ethanol	Ethanol	0,008	1000	0,16	0,525	145946	478825	0,0026	0,0904	0,0165	45,92
2b	max_ethanol		0,414						0,128	4,522	0,117	6,49
3a	min_water	Water	0,004	1000	0,16	0,525	267924	879016	0,0062	0,218	0,0163	34,45
3b	max_water		0,186						0,308	10,89	0,115	4,87

The results obtained for the test points for displacement expanders displayed in Table 3.2 are represented in the charts in Figure 3.6 for displacement expanders and Figure 3.7 for turbine expanders.

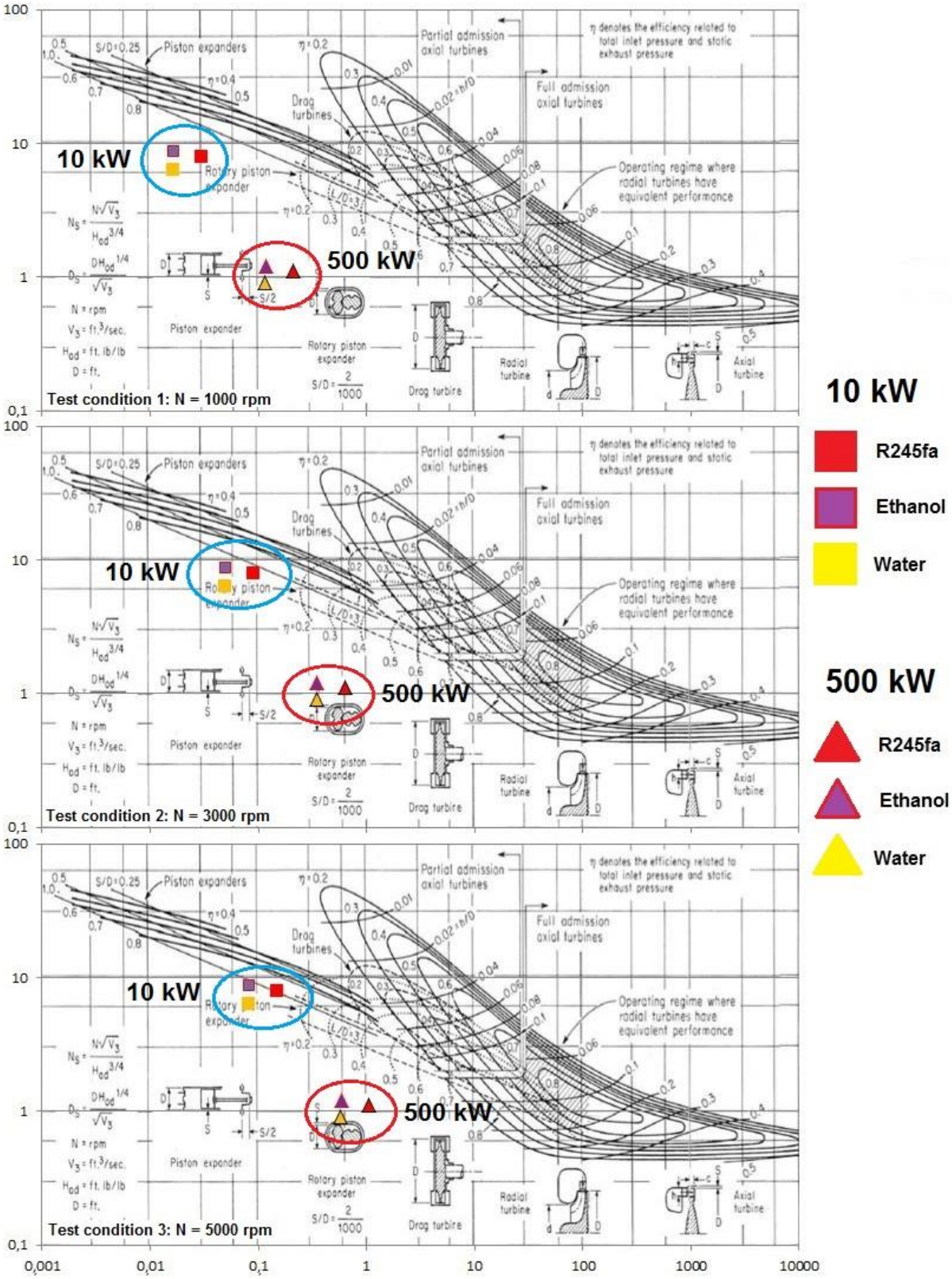

Figure 3.6 – Top: Test condition 1; Center: Test condition 2; Bottom: Test condition 3 (see Table 3.2), corresponding to the displacement expanders rotary speeds and a diameter of 0,03 m.

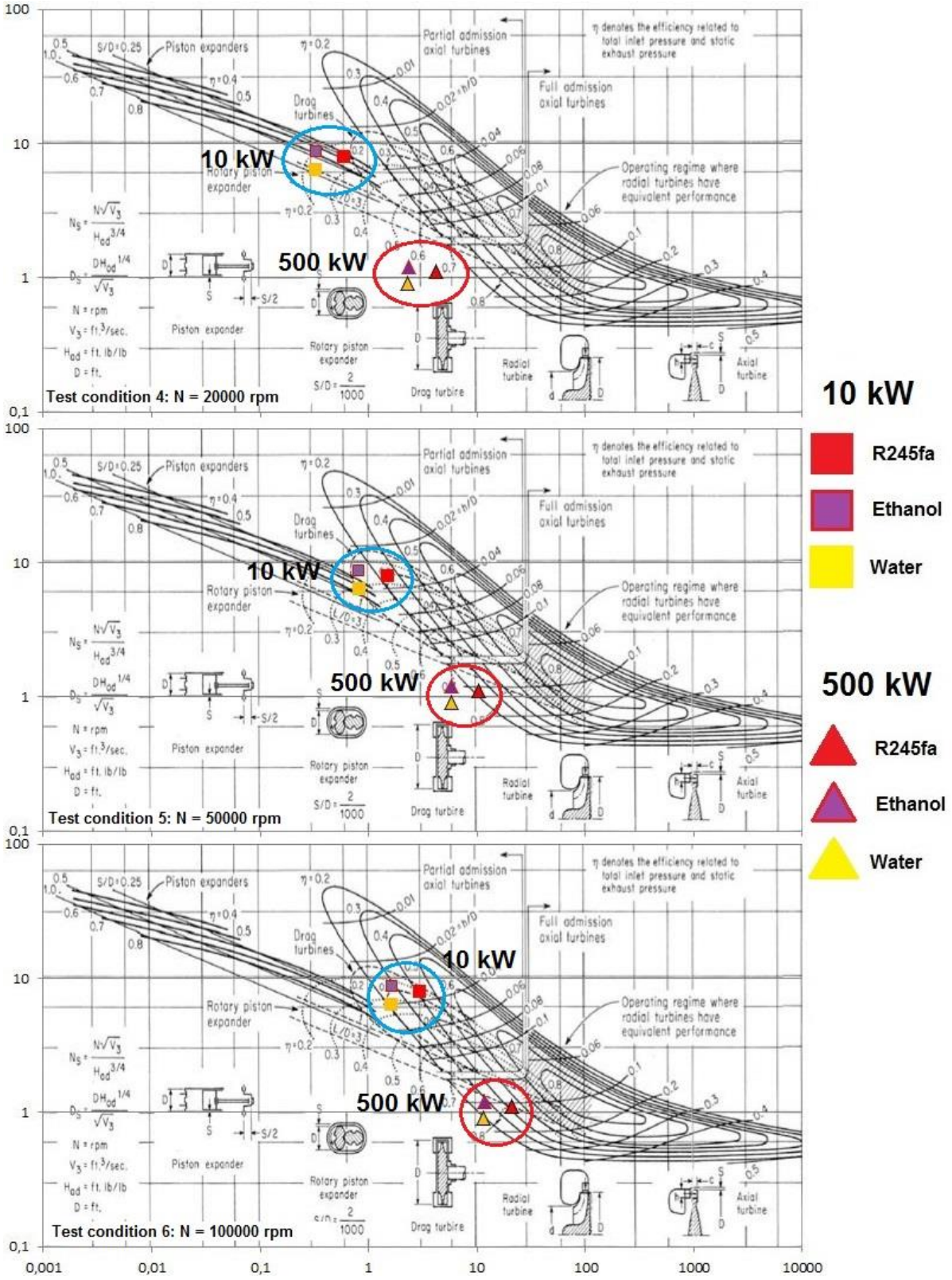

Figure 3.7 – Top: Test condition 4; Center: Test condition 5; Bottom: Test condition 6 (see Table 3.2), corresponding to the turbine expanders rotary speeds and a diameter of 0,03 m.

The points obtained in Figure 3.6 and Figure 3.7 show that a higher evaporator power is associated with a larger expander, and that a low evaporator power is associated with a smaller expander diameter. This also means that higher mass flow rates require bigger expanders, and lower flow rates require more compact expanders.

From Figure 3.6 and Figure 3.7 it is possible to observe that for the given diameter of 0,03 m, only test conditions 5 and 6 are obtained inside an expander type region – which means that for the given diameter, only turbines working under high rotational speeds should be selected. Besides, only in point 6 all the 3 fluids are simultaneously inside that area, as for point 5 only R245fa is inside the turbine region. In point 4, raising the rotational speed to a slightly higher value may result in that the point is obtained inside the turbine region.

3.4.1. Influence of the expander's diameter

To evaluate the influence of the expander diameter on the NsDs expander chart, it was tested an expander used by the authors Daccord *et al.* (2014) that has a piston diameter of 160 mm (0,160 m). Note that, the expander diameter used in the selection procedure presented in the previous section has 0,03 m (see Table 3.2). As a result, the N_s and D_s values will be recalculated using this diameter value (0,16 m) to determine the influence it has in the expander NsDs chart. The results are shown in the Appendix 1.

The figures in the Appendix 1 show that a bigger diameter makes the displacement expanders suitable for selection for the given conditions. In point 1, all 3 fluids are a good solution, especially for lower evaporator power (the points closer to the expander region where obtained with the lowest evaporator power of 10 kW), while in point 2 they are all suitable for a higher evaporator power (closer points were obtained with 500 kW). As for point 3, water and ethanol still are good solutions if combined with displacement expanders, while R245fa already reveals a better combination with turbine expanders. Both points 4 and 5 show that all fluids are suitable for a turbine expander for the tested conditions, and the same happens in point 6 for high evaporator powers.

3.4.2. Expander selection for the present study

The expander used in the experimental setup used for this study was a swash-plate piston expander, and the setup information can be found in Galindo *et al.* (2015). The suitability of the expander in this experimental setup will be verified in this section, and the points studied are depicted in Table 3.5, Galindo *et al.* (2015).

Table 3.5 - ORC operating points for simulation in Galindo *et al.* (2015).

	Unit	OP 1	OP 2	OP 3	OP 4	OP 5
Boiler Power	[kW]	5	12	20	25	30
High Pressure (evaporator)	[bar]	14,8	15,7	18,7	24	24,8
Low Pressure (condenser)		2,3	1,9	2	2,5	2,5
Mass flow rate	[kg/h]	16,67	39,95	64,95	82,01	102,87
Expander Speed	[rpm]	1018	2527	3511	3021	3354
Expander Torque	[Nm]	2	2,7	3,5	5	5,2
Expander Power	[kW]	0,21	0,71	1,28	1,58	1,83

The boiler power was not considered for each point individually. The calculations were performed considering a boiler power between a minimum of 5 kW and a maximum of 30 kW for all points, which will result in a region covered by the same point. The results are presented in the Figure 3.8 and Figure 3.9.

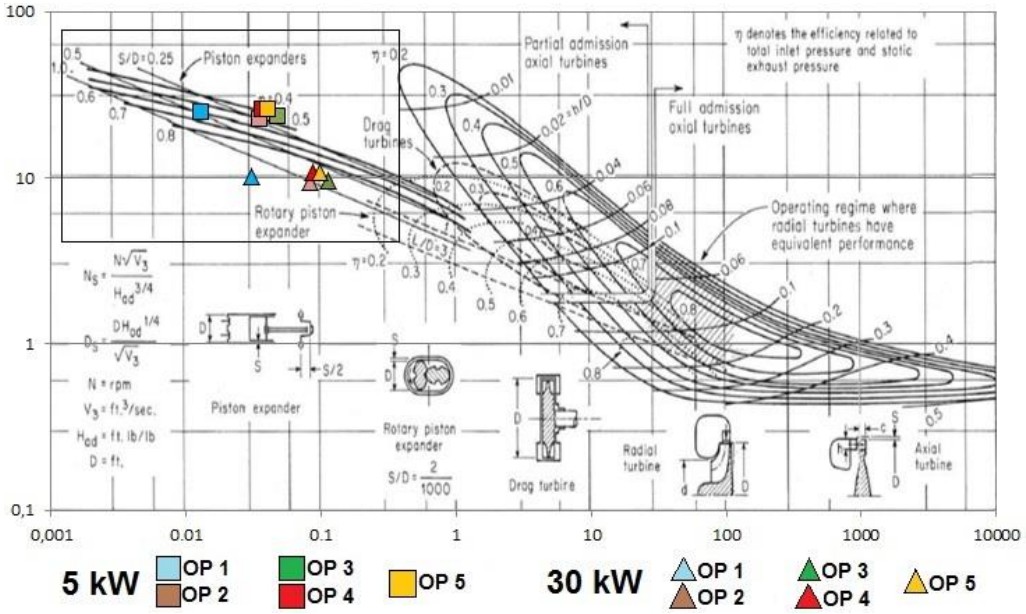

Figure 3.8 - Region obtained from the experimental data in the NsDs chart.

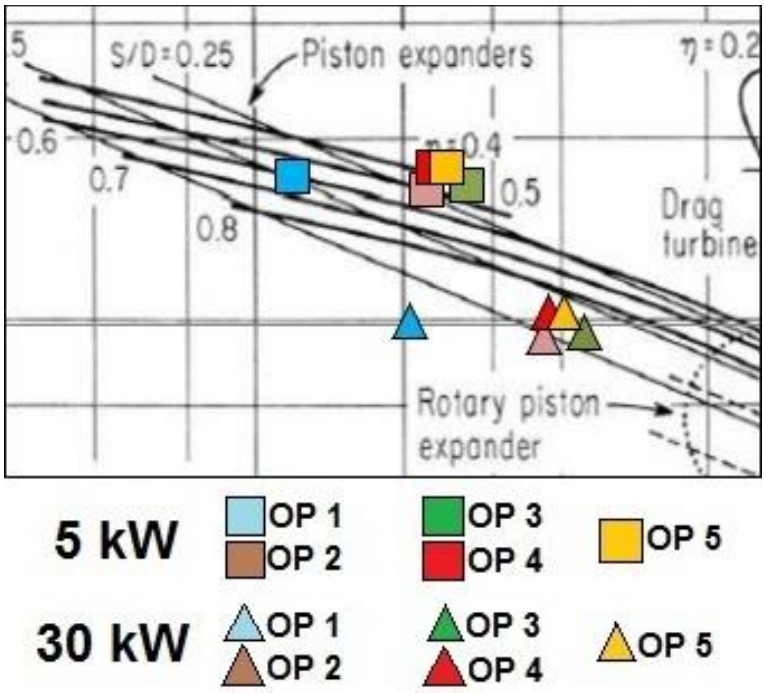

Figure 3.9 – Zoom of the region obtained in the NsDs chart from the experimental data.

The region obtained confirms that a piston machine is the best type of expander for the experimental setup, for the given conditions. All the five operating points cover the piston expander region, for the given system characteristics.

3.5. Summary

The results confirm the accuracy of the calculations, since the regions obtained in the charts match the expanders previously selected. One of the conclusions that can be taken beforehand is that the NsDs expander chart may be used to find the adequate expansion machine for a given application according to the region obtained, and not a specific application point. This is due to the proximity of the obtained points and the fact that the chart has logarithmic scales in both axis, which combined make the results inaccurate.

Obtaining a region inside a type of expander in the chart means that that type of expander is the most suitable for that given application. The combination of the N_S with the D_S results in that a lower diameter of the expander will have to be combined with an increase in the expander rotational speed, and for low speeds the diameter will have to be bigger. This means that high speeds and low diameters will mostly result in the turbine region and low speeds combined with higher diameters will result in the displacement expander area. Given this, it can be confirmed that turbine expanders are more compact than displacement expanders.

The expander selected for the experimental setup, Galindo *et al.* (2015) was a swash-plate piston expander. According to the calculations performed in this chapter, the most suitable expander type for the system is a piston expander, which means that the expander in use is adequate.

An important observation is also the fact that the working fluids' influence in the region is not actually very significant, but the R245fa is positioned at the right of the other fluids in the chart for low speeds, which means that is closer to the turbine region than water or ethanol – from the 3 fluids, it is the only one suitable for using in combination with turbines for being a dry fluid. This conclusion is important to the fact that combining a fluid with an expander must not be done only according to the characteristics of the system and the NsDs chart, but also according to the characteristics of the fluid and how they may affect the reliability of the expander selected.

4. The expander model

4.1. Introduction

The expander model was developed and validated against experimental data obtained at the *Centro de Motores Térmicos* (CMT) of the Polytechnic University of Valencia. The experimental setup can be found in Galindo *et al.* (2015). The goal is to obtain results as close as possible to the experimental runs in order to avoid the expensive and long runs in the future.

First in this chapter, in section 4.2, there will be a description of the schematic models found in literature, in order to have a theoretical approach to the model developed. Then, in section 4.3, information will be provided about the available softwares that are commonly used in the section as well as their main characteristics. Section 4.4 contains the description of the final model and the assumptions made. There is a step-by-step explanation and then a detailed model description, with all the main components explained. Section 4.5 provides the input parameters that can be already added to the software, taking into account that most of the values are given by the final results of the experimental runs. Finally, in section 4.6, the model is validated.

4.2. Different model types

Three types of models can be distinguished: empirical (black-box); semi-empirical (grey-box); deterministic (white-box), Lemort (2013). An empirical (black-box) model is characterized by very low computational time and high numerical robustness, does not allow extrapolation beyond calibration range and is suitable for dynamic simulations of RC systems. In resume, this model allows to simulate the expander as a black box with specific boundary conditions at the inlet and outlet. A semi-empirical model is usually used for steady state simulations, and allows the variation of the operating conditions and mechanical characteristics due to the fact that those conditions are known, such as: supply and exhaust pressure losses, internal leakages, mechanical losses, heat losses to the ambient and under and over expansion or compression losses. A deterministic model goes

even further and describes the expander with differential equations of conservation of mass and energy, and is used for optimizing the expander's design.

A semi-empirical model on a reciprocating expander was developed by Glavatskaya *et al.* (2012). The schematic representation of the model can be seen in Figure 4.1.

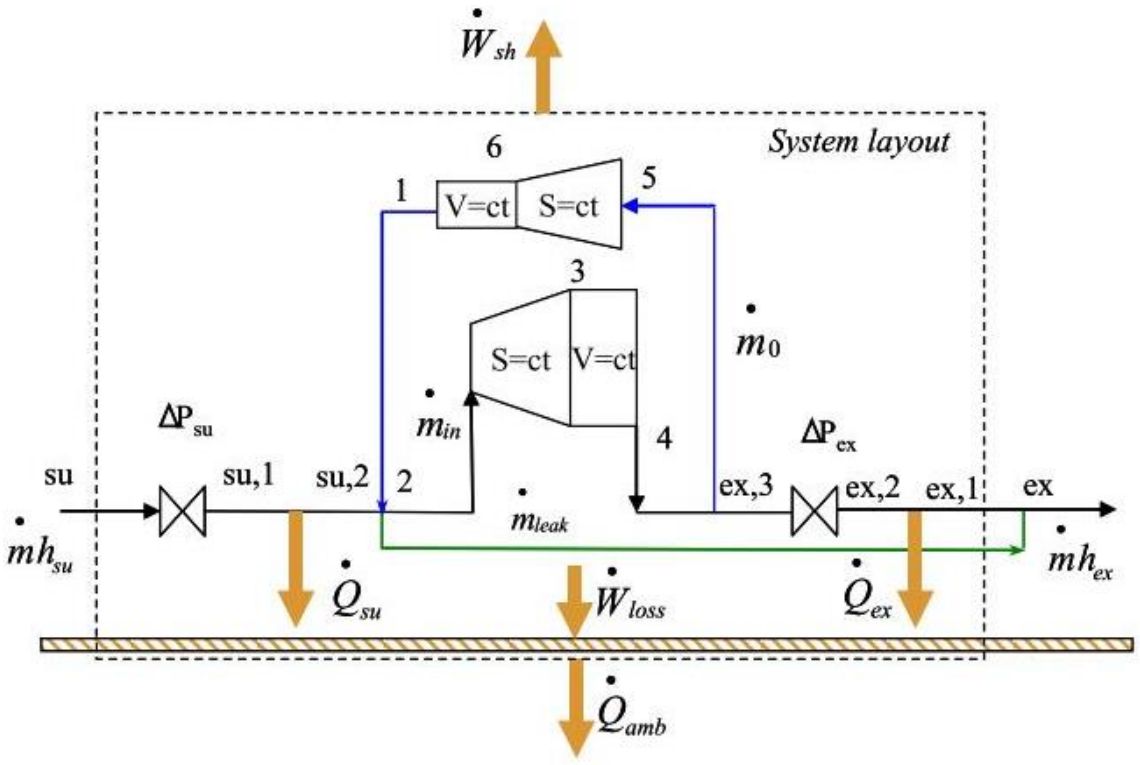

Figure 4.1 - Schematic representation of the expander model found in Glavatskaya *et al.(* 2012).

In the schematic representation depicted in Figure 4.1, all the steps through which the fluid goes from the inlet to the outlet of the expander are represented, and the steps are:

- ΔP_{su} $(su \rightarrow su, 1)$ corresponds to the pressure loss that occurs during the suction process;
- $\dot{Q}_{su}$ $(su, 1 \rightarrow su, 2)$ corresponds to the cooling process that occurs by the contact of the working fluid with the metal housing;
- 2,3,4 represents de expansion process, considering an isentropic expansion $(s = cte)$ and an expansion at constant machine volume $(V = cte)$;
- 5,6,1 represents de compression of the residual working fluid mass trapped inside the cylinders at the end of the discharge process;

- ΔP_{ex} $(ex, 3 \rightarrow su, 2)$ corresponds to the pressure loss at the exhaust of the expander;
- $\dot{Q}_{ex}$ $(ex, 2 \rightarrow su, 1)$ corresponds to the heating that occurs by the contact of the cooled working fluid with the heated housing;
- $\dot{W}_{loss}$ corresponds to the mechanical losses;
- $\dot{Q}_{amb}$ corresponds to the heat losses from the system to the ambient air.

A more detailed explanation of the scheme and all the variables can be found in literature Glavatskaya *et al.* (2012), Lemort (2013).

Due to the impossibility of determining the thermal losses, pressure losses and mechanical losses separately, as well as the residual fluid left in the chamber that will also cause a loss in the compression process, the model developed in the present work will be empirical (black-box). All the parameters known for modelling the expander are external to the box depicted in the Figure 4.2 that presents the inlet and outlet working fluid conditions, rotary speed, volume of the cylinders and opening and closing angles of the valve and port.

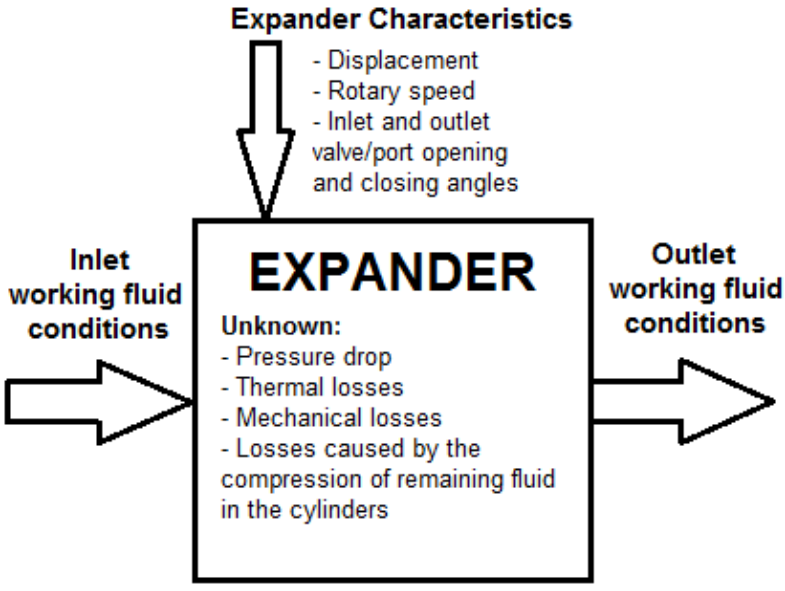

Figure 4.2 – Empirical (black-box) model of the expander modeled for this work.

4.3. Softwares available

Table 4.1 shows a summary of the main softwares used in previous similar studies and their usage in each study.

Table 4.1 – Softwares used by authors in previous studies.

Software	Type of study	Authors
EES	- Semi-empirical simulation models of 3 different expansion machines	Legros *et al.* (2014)
	- Steady-state semi-empirical model of an expander device	Glavatskaya *et al.* (2012)
EES and F-Chart Software	- Model for a binary power cycle considering realistic condensing ORC cycles for geothermal applications	Sauret & Rowlands (2011)
REFPROP	- Fluid properties calculator	Wang *et al.* (2011), Arunachalam *et al.* (2012), Legros *et al.* (2013), Katsanos *et al.* (2010)
AMESim	- Development ORC simulation model	Ziviani *et al.* (2012)
	- Swash-plate pump detailed model and simulation	Drupal & Nupet (n.d.)
Matlab	- Model development	Wang *et al.* (2011), (Legros *et al.* (2013)
	- Numerical solutions and graphs	Grip (2009)
Other (Non Specified)	- Turbine and double action piston machine models using a commercial 1D-system simulation tool	Seher *et al.* (2012)
	- CAD model of a prototype of a single-stage impulse turbine of realistic size and weight	Kunte *et al.* (2013)

The Engineering Equation Solver (EES) is a very powerful tool in terms of thermodynamic properties calculation and prediction as it provides a very complete database of fluid properties, making it easy to use by just input the equations and the values required to compute the solution. It also gives the possibility of drawing parametric tables in order to obtain various results for different system conditions, so that graphics and maps can be obtained for a great number of different machines and working fluids. Legros *et al.* (2014) used the EES to model, simulate and compare 3 different expanders.

REFPROP (Reference Fluid Thermodynamic and Transport Properties Database) is also a very complete thermodynamic properties calculator, and was developed by the National Institute of Standards and Technology (NIST) of the United States of America. It can be used to calculate the properties of several working fluids, and can also be interfaced with other softwares, for example Matlab, Wang *et al.* (2011) or, in the case of this work, Excel (chapter 3).

LMS Imagine AMESim (Advanced Modeling Environment Simulator) was the software used in the present work, is a very complete engineering software, with an extended library, also including an extreme list of working fluids, that can be used to model several different systems (form small air-conditioning components to complex mechatronic systems). It allows the simulation of systems under transient and stationary operating conditions, with specified control strategies. It is adequate for ORC system modeling and simulation, and for these reasons it was chosen for the present work.

Matlab is a numerical computing environment and a programming language. It can be used to compute the pressure-volume (PV) diagrams, from the data obtained experimentally, and to compare it to the diagrams obtained from the AMESim model. It was used in this work to compare the PV diagrams obtained experimentally with the PV diagrams obtained with AMESim, in order to adjust and calibrate the model, and also to determine the accuracy error of the model.

4.4. LMS Imagine AMESim

AMESim is a 1D (one-dimensional) software that allows simulations of various engineering systems. It is based on an intuitive graphical user interface in which the system is displayed throughout the simulation process. The model is implemented by connecting

the components, in order to model the desired engineering system. The components are represented through standard symbols used in the engineering field (such as ISO). In the case that such standards don't exist, the components are displayed through a pictorial representation that is easily recognizable by the user. Each component has a number of ports for connection between them, and when a connection is not possible, the software blocks the connection, making it also user friendly in saving time in finding errors in the system connections.

The software AMESim is a very powerful tool that can replace the long and expensive experimental runs of complex systems, with accuracy and precision, in order to optimize the overall system, or to optimize some specific parts or components.

The wide range of libraries, divided in a large amount of categories, gives the possibility to perform simulation runs both in simple and complex systems. They go from signal control, mechanical, thermal or two-phase flow, to vehicle dynamics, automotive electrics or aircraft & space, among many others.

The default interface of the AMESim interface and libraries is shown in Figure 4.3.

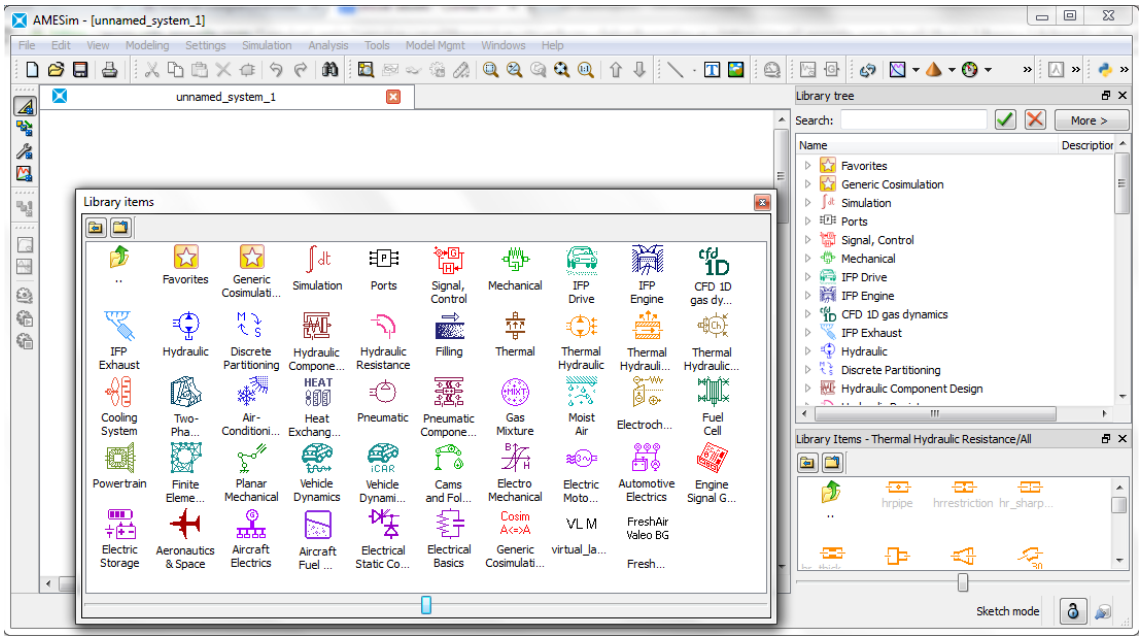

Figure 4.3 – Amesim interface and libraries

The standard library has three categories:

- **Simulation** - provides submodels related to the integration of systems and numerical utilities used by other libraries. It components for analyzing statistics of runs, setting simulation parameters, print intervals, interactive components and for 3D models;
- **Signal, Control** – gives the possibility to construct block diagram models, which represent dynamic physical systems graphically, and can also be used to generate complex signals to pilot physical systems;
- **Mechanical** - offers a large set of basic mechanical components, which allow the user to model various dynamical 1D mechanical systems. It is able to handle a large number of applications, from the simple motion of a rotary load to complex phenomena such as friction or collision.

The appendix 1 presents the extra libraries that are used to design the overall system, defining the type and complexity. More than one category can be used in the same system.

AMESim also gives the user the chance of having master-slave groups of systems. For example, a common rail injector system can be found in the help option (that will be described further in this subchapter), has the main fuel lines in the master sketch and then the pump and the 4 injectors are modeled in other 5 sketches. The sketches are connected through senders and receivers found in the "*Signal, Control*" library.

The help option provides an immense amount of detailed information. It can be used in a single component to know its description, usage, variables (external and internal), and look for sketches and equations. In case it is used to compute any data or perform any type of calculations – some components may be able to perform more than one calculation. It can also be used to find explanatory information about complete circuits and systems, and it even provides files with examples of systems for certain applications, that can be downloaded by the user and loaded into the AMESim for running and obtaining results.

4.5. Developed expander model

The model developed and implemented in the present work consists on a piston and a variable volume chamber, as shown in Figure 4.4. The libraries used were the two-phase flow (dark blue), signal control (red) and mechanical (green). Drupal & Nupet (n.d.) present a model similar to the model developed in this work.

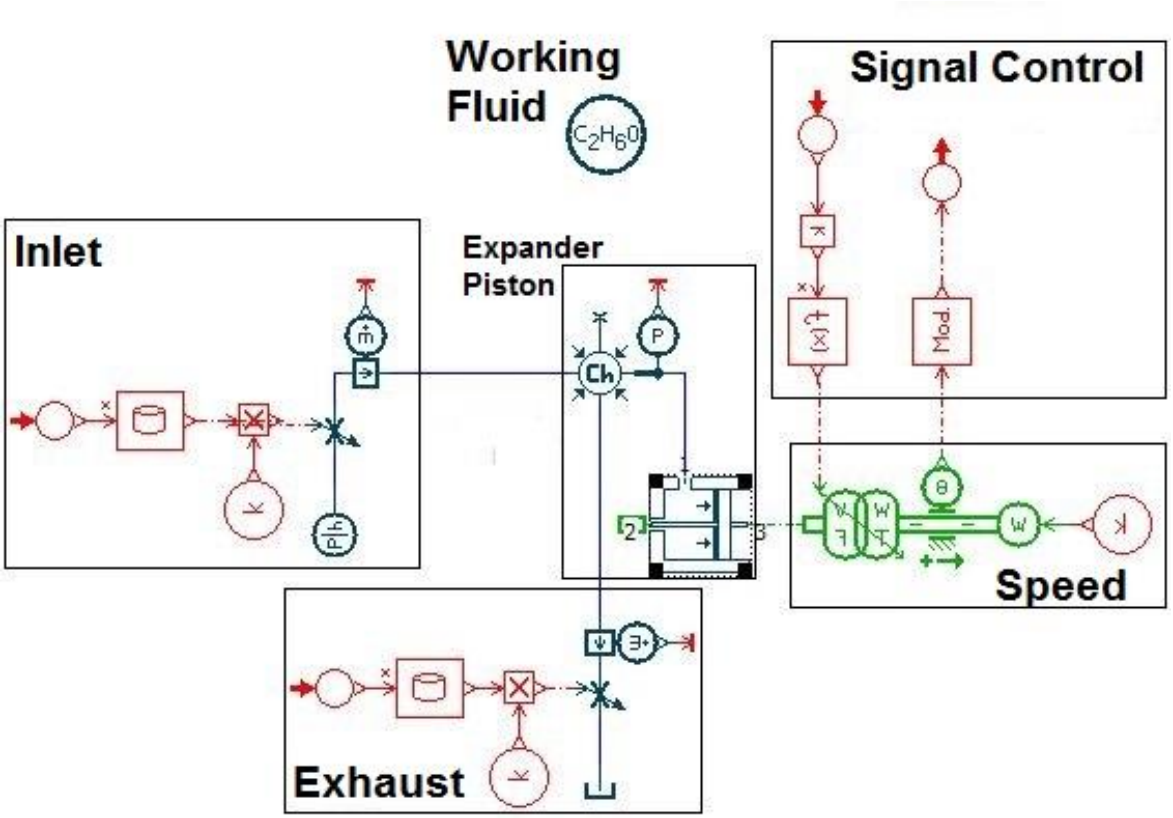

Figure 4.4 – AMESim expander model developed in the present work

The boxes depicted in the sketch provided in the Figure 4.4 show which group of components are used to model the different parts of the expander. Specifically, the working fluid inlet and outlet conditions are inserted in the inlet and exhaust boxes, respectively. The expander speed is inserted in the speed box. The valves opening and closing are determined by the signal control box, and the piston characteristics are inserted in the expander piston box. With the detailed explanation of the modeling process in this chapter, the components will be explained and displayed in tables.

For the input parameters, there is a constant signal with a specified value for the rotary speed and two sources for the inlet and exhaust of the piston. While the rotary speed

is input as a dimensionless value and then converted to rotary speed (reviews per minute), the sources for inlet and exhaust are initialized from two different thermodynamic variables (from 4 possible combinations). In this model, the chosen combination was temperature (T) and pressure (P). Components for the input parameters are described in Table 4.2.

Table 4.2 – Components for the inputs

Graphical Representation	Component Name	Brief Description
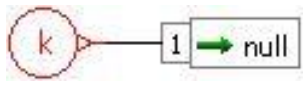	CONS00	Constant value input. Used to insert the rotary speed.
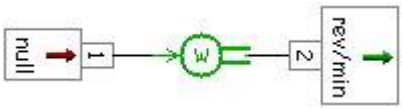	OMEGC0	Converts the constant input signal to rotary speed.
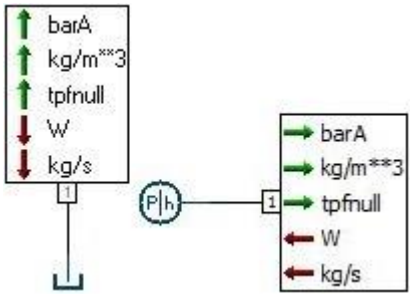	TPFCPHS000	Constant pressure and enthalpy sources. The type of initialization is selected as pressure and temperature. There are two different visual drawings with no thermodynamic difference.

The opening of the inlet and exhaust valves is controlled by the components given in Table 4.3. An angular displacement sensor (TPFCPHS000) reads the input rotary speed and sends it to a function submodel (MOD00), that converts the rotary speed into an angle between 0 and 360 degrees. After the conversion, the signal goes through a table input submodel (SIGFXA01) to be converted from the value of the angle to a value between 0 (totally closed) and 1 (totally open). It is then sent to a flow restrictor (TPFMGR00), that works as a pressure drop valve, to change the area of the pipe following the next equation:

$$Area = signal \times Area_{Max} \tag{18}$$

A direct connection between the table input component and the pressure drop valve components is not possible, so a signal multiplier (MUL00) will be added to the sketch for

connection purpose only. This component requires a constant signal input, so the unit value will be inserted. Besides, to avoid having lines through the sketch, which would make it more confusing, the connection between some components is made through signal transmitters (SIGTRANS0) and receivers (SIGRECEI0).

Table 4.3 – Components for computing the valve and port opening and closing.

Graphical Representation	Component Name	Brief Description
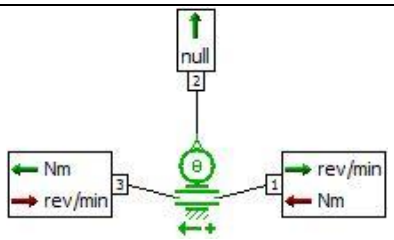	TPFCPHS000	Angular displacement sensor. Computes de angular displacement in degrees by integrating the angular velocity.
	MOD00	Limits the angle interval to be [0,360].
	SIGTRANS0	Signal transmitter. Sends the signal to one or several receivers without visible sketch lines.
	SIGRECEI0	Signal receiver, linked to a transmitter for an invisible connection.
	SIGFXA01	Table input. Used to interpolate the values of the opening and closing of the inlet and exhaust valves
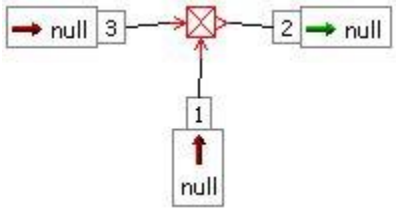	MUL00	Signal multiplier. Used only for connection between the table input and the pressure drop valve. The input signal provided in port 1 is unitary.
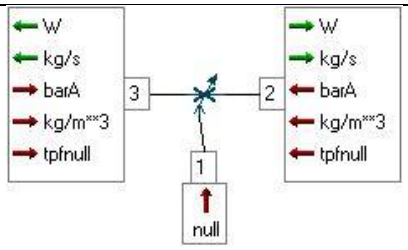	TPFMGR00	Two-phase flow restrictor. Used as a pressure valve to compute a pressure drop for both laminar and turbulent conditions.

Then, the rotary speed of the expander needs to be converted to the linear speed of the piston. The first component to be added is a gain component (GA00) that is inserted after the signal receiver to convert the received angle from degrees into radians (the software works in radians).

The conversion from rotary speed into linear velocity is then computed, by means of a rotary-linear modulated transformer (WTX03), which receives the rotary speed in one port and the angle converted in the gain component to compute the linear velocity of the piston. The conversion is calculated by the following equation:

$$v = l \times w \times c_1 \tag{19}$$

The output linear velocity (v, in m/s) is the product of the angular speed (w, in rad/min) and the transformer ratio (l). c_1 is the conversion factor used to convert from angular velocity to linear velocity ($2\pi/60$).

The transformer ratio (l) is the linear displacement (none constant, since it changes proportionally to the rotation of the swash plate), that has to be input by the user directly in the function input submodel (FX00) that has to be added before the transformer, in which the relation is shown in equation 23. Figure 4.5 presents the scheme used to determine the transformer ratio (l).

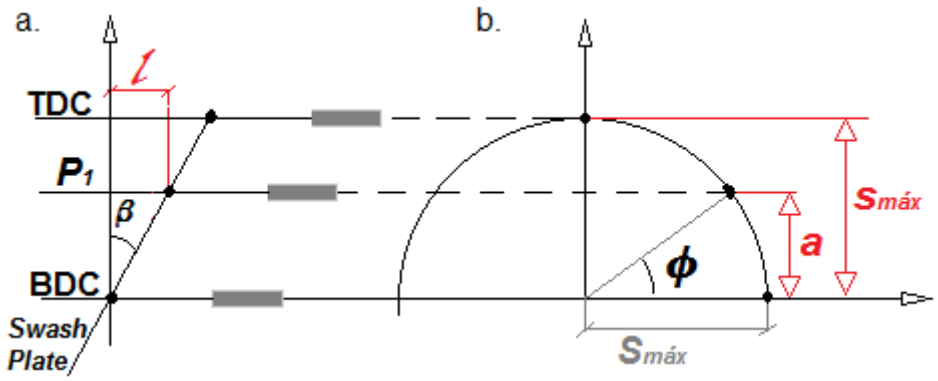

Figure 4.5 – Scheme used to determine the transformer ratio (l); a) Side view of the Swash Plate; b) Top view of the swash plate.

As can be seen in Figure 4.5a), P_1 is the point that corresponds to the position of the piston at a given moment, in the swash plate. That position is constantly changing from the BDC (Bottom Dead Center, the initial position) to the TDC (Top Dead Center, the final

position), and back to the BDC, and can be transposed from a side view to a top view (Figure 4.5a) and Figure 4.5b)). Figure 4.5a) corresponds to the side view of the swash plate, in which β is the angle of the swash plate (fixed) and l is the linear displacement of the piston for a given P_1. Figure 4.5b) is the top view of the swash plate, where ϕ is the angle that P_1 does with the BDC, $S_{máx}$ is the stroke of the piston and a is also a distance that P_1 does with the BDC, but used for calculation purposes only.

Given this, a system of 2 equations can be obtained and solved, which permits to obtain the transformation ratio (l):

$$\begin{cases} sin(\phi) = \dfrac{a}{S_{máx}} \\ tan(\beta) = \dfrac{l}{a} \end{cases} => \begin{cases} a = sin(\phi) \times S_{máx} \\ l = a \times tan(\beta) \end{cases} => l = S_{máx} \times tan(\beta) \times sin(\phi) \qquad (20)$$

This function uses the angle coming out of the angle sensor (TPFCPHS000, see Table 4.3), multiplies it by the correspondent angle of the piston position (β), and the radius of the swash plate.

Table 4.4 presents the components used to convert the rotary speed into linear velocity.

Table 4.4 – Components used to convert the rotary speed into linear velocity.

Graphical Representation	Component Name	Brief Description
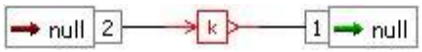	GA00	Gain component. Used to input a function to determine the rotary speed from the given angles.
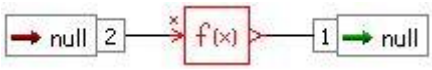	FX00	Output function of one variable. Computes the transformer ratio required to convert the rotary to linear speed.
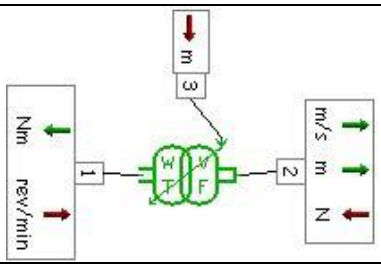	WTX03	Rotary-to-linear modulated transformer. Converts the rotary speed of the expander into the linear speed of the piston.

For the piston expander box (see Figure 4.4), there are two important components: the Volume Chamber (TPFBHC11) and the Piston (TPFBAP12). Table 4.5 presents the components used to model the piston chamber. The Volume Chamber has variable volume, temperature and pressure, and is used to compute the mass flow rate of the working fluid from the values input in all four ports, as well as the volume of the piston chamber. The inputs for the Piston component are: the piston diameter, rod diameter and the minimum length of the chamber (length at zero displacement).

Table 4.5 – Components used to model the piston chamber.

Graphical Representation	Component Name	Brief Description
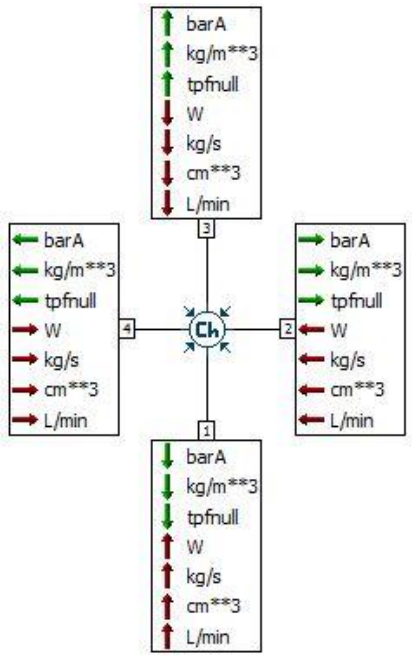	TPFBHC11	Volume chamber. Computes the mass flow rate, density and enthalpy of the fluid, the volume of the piston chamber and the pressure inside the chamber.
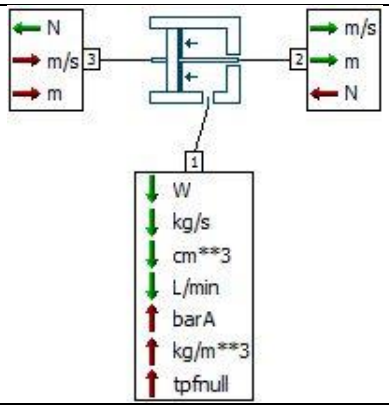	TPFBAP12	Piston Component. Uses the velocity and force as inputs in order to compute the length and volume of the chamber and the pressure.

As for the sensors found in the model, they are used solely for the purpose of checking the values of the mass flow rate calculated from the constant signal inputs (both the inlet and exhaust), and the pressure given by the piston submodel. They have no influence in the circuit.

The Refrigerant Properties submodel (TPF_FP01) provides a complete database of fluids and refrigerants to select as the working fluid, computing the specific heat at constant pressure, absolute and kinematic viscosities, specific enthalpy, etc. Table 4.6 presents the component used to select the working fluid of the model.

Table 4.6 – Component used to select the working fluid of the model.

Graphical Representation	Component Name	Brief Description
	TPF_FP01	Refrigerant properties. Used to define the ethanol (C_2H_6O) from the database given.

After modeling the system depicted in Figure 4.4, the input parameters required are:

- The index of the fluid;

- The temperature and pressure of the fluid at the inlet and outlet ports;

- Rotary speed of the expander;

- Piston diameter and rod diameter for the piston submodel;

- Tables for the inlet and outlet valve/port opening and closing angles.

4.6. Model validation

The results obtained by the implemented model were compared against the experimental data, in order to adjust the model so that it could have predictable results. The five points used in this study (see Table 3.5) were obtained through static runs, Galindo *et al.* (2015).

The system under investigation considers ethanol (C_2H_6O) as working fluid. For the simulations and the resulting PV graphs were compared with the ones extracted from the instant pressure center inside the cylinder, using Matlab.

The piston submodel demands its diameter and rod diameter, and also the chamber length at zero displacement (these values were provided by the expander manufacturer). For the variable volume submodel it is only necessary to define the dead volume.

Due to confidentiality reasons, the values used for the model runs, as well as the results obtained, must be omitted. For that reason, only the points found in Galindo *et al.* (2015) will be used to explain what results and how they can be obtained with the model developed in the present work.

Table 4.7 – Experimental data used for AMESim model validation.

Test Point	P_{in} [bar]	T_{in}* [ºC]	P_{out} [bar]	T_{out}** [ºC]	N [rpm]	D [mm]
1	14,8		2,3	114,83	1018	
2	15,7		1,9	103,77	2527	
3	18,7	200	2	96,56	3511	30
4	24		2,5	111,20	3021	
5	24,8		2,5	109,04	3354	

*** Imposed, was not available; ** Calculated from Excel, using REFPROP**

In the AMESim, the points are tested in batch runs so they can be tested simultaneously: batch parameters is an option that allows to run several points at once, saving time and simplifying the process. The batch is created when in simulation mode, in the settings option. Then the submodels in which the parameters will be inserted have to be dragged (Figure 4.6).

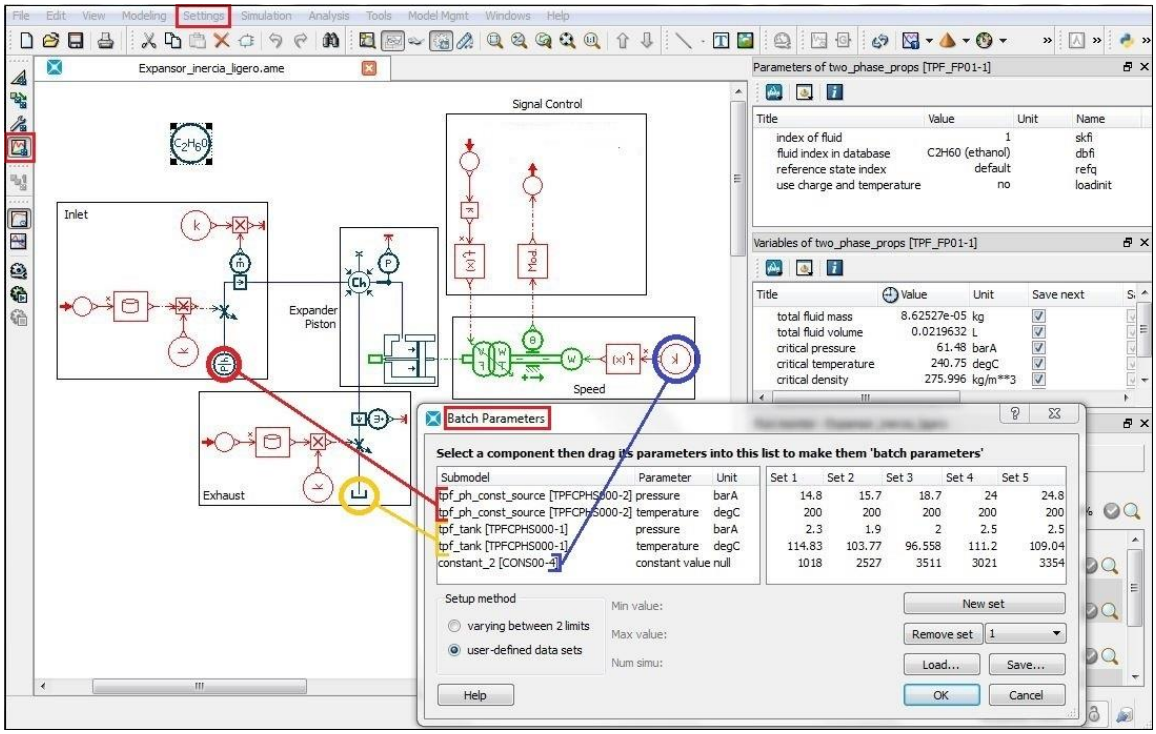

Figure 4.6 – Creating batch parameters for simultaneous runs.

From the piston, it is possible to extract the density of the fluid, the volume displaced per second (derivative of volume), the linear velocity of the piston, the force on the piston and the work (enthalpy flow rate). From the volume chamber, the mass flow rate, specific enthalpy and gas mass fraction of the fluid can be extracted.

The results can be shown graphically. PV graphs were extracted and saved as data files (.dat), so they could be loaded into Matlab in order to be compared with the PV graphs obtained through the data obtained experimentally. The error of the model results were determined to be approximately 5%.

The difficulties of modeling lied mostly on the connections of some components: the connection between the table (SIGFXA01) and the flow restrictor (TPFMGR00) was not possible, requiring the use of an intermediate component with no use for the model to perform the connection (signal multiplier, MUL00) (see Table 4.3). Also, the opening and closing angles of the valves required precise data that could only be provided by the manufacturer. With a default exponential table was only possible to obtain graphical results with a low level of detail. The results were also not accurate and the error between the experimental results and the model results did not follow a pattern. Also, this was causing the software to calculate the results while changing the input temperature variable to a value approximate to the selected in some of the test points, making them unreliable.

5. Conclusions

Given the importance of the expander machine on the RC system's efficiency the present work is focused on the modeling of a Swash-plate Piston Expander for an ORC system using the AMESim software in order to compare it with real run simulations.

The results revealed that low rotational speeds should be associated with larger expander diameters, which indicates that, for this combination, the displacement expanders are the most adequate. As for high rotational speeds, that are characteristic of turbine expanders, they must be associated with low diameters, in order to suit in automotive applications. Given this, turbines might be the best solution in ORC systems for small vehicles, taking into account spatial and weight requirements.

The expander selected for the experimental setup, Galindo *et al.* (2015) was a swash-plate piston expander. According to the calculations performed in this chapter, the most suitable expander type for the system is a piston expander, which means that the expander in use is adequate.

The fluid selection did not reveal a significant influence in terms of selecting an expansion machine according to the NsDs expander chart, since all the points obtained for all the fluids are not very distant from each other. So, in conclusion, the expander machine shall be selected according to the fluid suitable for the given system (hot and low temperature sources.

5.1. Future works

The system designed in this work does not include heat or mechanical losses, considering that they were not measurable. In an expander with all the technical data detailed, in which is possible to know the friction losses and the material and thickness of the cylinder walls, it might be possible to revise the model in this work including all those losses.

The sequence of the calculations used to determine the position of the expander in the NsDs chart can be used in the reverse way to determine the conditions of the system according to a specific given expander, in case the system is built around the expander. In

this work, the sequence was developed to determine which expander suits better for the general default conditions of the RC systems up to date. In future works, the sequence can be adapted in order to achieve a specific interval of specific speed or specific diameter so that the pump power required for raising the fluid's pressure to a certain value or the evaporator power to heat the fluid into a required temperature can be determined. The most suitable fluid can also be selected using these calculations, if for example there are spatial restrictions for the system.

References

Arunachalam et al., 2012. Waste Heat Recovery from Multiple Heat Sources in a HD Truck Diesel Engine Using a Rankine Cycle - A Theoretical Evaluation. Available at: http://www.sae.org/technical/papers/2012-01-1602 [Accessed January 7, 2015].

Berger, 2014. Utilization of waste heat with the Clausius Rankine Cycle (CRC) in industry and transportation as a close-to-production SteamDrive. *4th Conference of Thermoeletrics, Berlin*.

Bosch, 2012. Diesel Systems Waste Heat Recovery System (WHR System) for commercial vehicles.

Bureau of Energy Efficiency, 8. WASTE HEAT RECOVERY. , pp.173–189. Available at: http://www.beeindia.in/energy_managers_auditors/documents/guide_books/2Ch8.pdf.

Cipollone et al., 2014. Mechanical Energy Recovery from Low Grade Thermal Energy Sources. *Energy Procedia*, 45, pp.121–130. Available at: http://linkinghub.elsevier.com/retrieve/pii/S1876610214000150 [Accessed January 7, 2015].

Clark, 2005. Non-Ideal Mixtures of Liquids. Available at: http://www.chemguide.co.uk/physical/phaseeqia/nonideal.html.

Daccord et al., 2014. Oil-Free Axial Piston Expander for Waste Heat Recovery. *SAE 2014 World Congress & Exhibition*.

Declaye et al., 2013. Experimental study on an open-drive scroll expander integrated into an ORC (Organic Rankine Cycle) system with R245fa as working fluid. *Energy*, 55, pp.173–183. Available at: http://linkinghub.elsevier.com/retrieve/pii/S0360544213003034 [Accessed January 7, 2015].

Dingel & Ambrosius, 2014. Development of Components for a CRP for Vehicle Applications. *4th Conference of Thermoeletrics, Berlin*, (December).

Dixon, 1977. Fluid mechanics, thermodynamics of turbomachinery. *International Journal of Heat and Mass Transfer*, 20, p.185.

Drescher & Brüggemann, 2007. Fluid selection for the Organic Rankine Cycle (ORC) in biomass power and heat plants. *Applied Thermal Engineering*, 27(1), pp.223–228. Available at: http://linkinghub.elsevier.com/retrieve/pii/S1359431106001475 [Accessed December 16, 2014].

Drupal & Nupet, Modeling of the different components.

Endo et al., 2007. Study on Maximizing Exergy in Automotive Engines. , (724).

EXOES, 2011. EXOES Rankine Technologies. Available at: http://www.exoes.com.

FChart, EES: Engineering Equation Solver. Available at: http://www.fchart.com/ees/.

Freymann et al., 2008. The Turbosteamer: A System Introducing the Principle of Cogeneration in Automotive Applications. *MTZ 05/2008 Vol 69: 20- 27, 2008.*

Galindo et al., 2015. Experimental and thermodynamic analysis of a bottoming Organic Rankine Cycle (ORC) of gasoline engine using swash-plate expander. *Energy Conversion and Management*, 103, pp.519–532. Available at: http://linkinghub.elsevier.com/retrieve/pii/S0196890415006470.

Glavatskaya et al., 2012. Reciprocating Expander for an Exhaust Heat Recovery Rankine Cycle for a Passenger Car Application. *Energies*, 5(12), pp.1751–1765. Available at: http://www.mdpi.com/1996-1073/5/6/1751/ [Accessed March 4, 2014].

Grip, 2009. *A mechanical model of an axial piston machine*,

Haller et al., 2014. Comparison of High and Low Temperature Working Fluids for Automotive Rankine Waste Heat Recovery Systems. , pp.1–9.

Hamilton & Hamilton, J., 2015. Diesel Engine Overload: Exhaust Gas Temperature.

Imelda, 2011. PassionWorld. Available at: https://imeldalee18.wordpress.com/2011/02/18/ethanolwater-azeotrope/.

Jadhao et al., 2013. Review on Exhaust Gas Heat Recovery for I . C . Engine. , 2(12), pp.93–100.

Kapoor, 2013. What is Turbo-compounding? Available at: https://www.quora.com/What-is-Turbo-compounding.

Katsanos, C.O. et al., 2010. Thermodynamic analysis of a diesel truck engine organic rankine cycle. , (July), pp.1–6.

Keneth, 1959. How to Select Turbomachinery For Your Application How to Select Turbomachinery For Your Application. *Barber-Nichols Inc.*

Kim et al., 2012. Optimization of Design Pressure Ratio of Positive Displacement Expander for Vehicle Engine Waste Heat Recovery. *Energies*, 7(9), pp.6105–6117. Available at: http://www.mdpi.com/1996-1073/7/9/6105/ [Accessed January 21, 2015].

Kunte et al., 2013. Partial Admission Impulse Turbine for Automotive ORC Application. Available at: http://www.sae.org/technical/papers/2013-24-0092 [Accessed January 7, 2015].

Langson, 2008. Energy Recovery From Natural Gas Letdown Stations. Available at: http://peswiki.com/index.php/Pressure_to_power.

Latz et al., 2012. Comparison of Working Fluids in Both Subcritical and Supercritical Rankine Cycles for Waste-Heat Recovery Systems in Heavy-Duty Vehicles. Available at: http://www.sae.org/technical/papers/2012-01-1200 [Accessed January 7, 2015].

Latz et al., 2013. Selecting an Expansion Machine for Vehicle Waste-Heat Recovery Systems Based on the Rankine Cycle. Available at: http://www.sae.org/technical/papers/2013-01-0552 [Accessed September 22, 2013].

Latz, 2013. *Waste Heat Recovery from Combustion Engines based on the Rankine Cycle*,

Legros et al., 2013. Investigation on a scroll expander for waste heat recovery on internal combustion engines.

Legros et al., 2014. Sizing models and performance analysis of volumetric expansion machines for waste heat recovery through organic Rankine cycles on passanger cars.

Lemmon et al., 2010. NIST reference fluid thermodynamic and transport properties, REFPROP version 9.1. Available at: http://www.nist.gov/srd/nist23.cfm.

Lemort, 2013. A Comparison of Piston , Screw and Scroll Expanders for Small - Scale Rankine Cycle Systems.

Lemort et al., 2009. Testing and modeling a scroll expander integrated into an Organic Rankine Cycle. *Applied Thermal Engineering*, 29(14-15), pp.3094–3102. Available at: http://linkinghub.elsevier.com/retrieve/pii/S1359431109001173 [Accessed November 13, 2014].

Lopes et al., 2012. Review of Rankine Cycle Systems Components for Hybrid Engines Waste Heat Recovery. Available at: http://www.sae.org/technical/papers/2012-01-1942 [Accessed November 4, 2013].

Macián et al., 2012. Methodology to design a bottoming Rankine cycle, as a waste energy recovering system in vehicles. Study in a HDD engine. *Applied Energy*.

Nikolov, Huck & Brimmer, 2012. Influence of Thermal Deformation on the Characteristic Diagram of a Screw Expander in Automotive Application of Exhaust Heat Recovery. *International Compressor Engineering Conference at Purdue, July 16-19*.

Oomori & Ogino, 1993. Waste Heat Recovery of Passenger Car using a Combination of Rankine Bottoming Cycle and Evaporative Engine Cooling System. *SAE paper 930880*.

Panesar et al., 2013a. An Assessment of the Bottoming Cycle Operating Conditions for a High EGR Rate Engine at Euro VI NOx Emissions. , 50. Available at: http://www.sae.org/technical/papers/2013-24-0089 [Accessed January 7, 2015].

Panesar et al., 2013b. Working fluid selection for a subcritical bottoming cycle applied to a high exhaust gas recirculation engine. *Energy*, 60, pp.388–400. Available at: http://dx.doi.org/10.1016/j.energy.2013.08.015.

Patel & Doyle, 1976. Compounding the truck diesel engine with an organic Rankine-cycle system. *SAE paper 760343*.

Quoilin et al., 2012. Working fluid selection and operating maps for Organic Rankine Cycle expansion machines. , pp.1–10.

Quoilin & Lemort, 2009. Technological and Economical Survey of Organic Rankine Cycle Systems.

Sankey Diagrams, Typical Energy Split in Gasoline Internal Combustion Engines. Available at: http://www.sankey-diagrams.com/wp-content/gallery/o_sankey_209/energy_split_combustion_engine.png [Accessed January 1, 2014].

Santos et al., 2011. Expander Selection For Internal Combustion Engines Bottoming With Steam And Organic Rankine Cycle.

Sauret & Rowlands, 2011. Candidate radial-inflow turbines and high-density working fluids for geothermal power systems. *Energy*, 36(7), pp.4460–4467. Available at: http://linkinghub.elsevier.com/retrieve/pii/S0360544211002441 [Accessed November 7, 2013].

Seher et al., 2012. Waste Heat Recovery for Commercial Vehicles with a Rankine Process.

Shoemaker, 2014. Discovering Electric Turbo Compounding (ETC). , 44(0).

Song et al., 2013. An investigation on the performance of a Brayton cycle waste heat recovery system for turbocharged diesel engines. *Journal of Mechanical Science and Technology*, 27(6), pp.1721–1729. Available at: http://link.springer.com/10.1007/s12206-013-0422-2 [Accessed December 23, 2014].

Stine & Geyer, 2001. Solar Energy Systems Design. Available at: http://www.powerfromthesun.net.

Tahir et al., 2010. Efficiency of compact organic rankine cycle system with rotary-vane-type expander for low-temperature waste heat recovery. *World Academy of Science, Engineering and Technology*, 4, pp.775–780.

Tan, 2005. BMW TurboSteamer. Available at: http://paultan.org/2005/12/11/bmw-turbosteamer/.

Teng et al., 2011. A Rankine Cycle System for Recovering Waste Heat from HD Diesel Engines - WHR System Development. Available at: http://www.sae.org/technical/papers/2011-01-0311 [Accessed January 7, 2015].

UNEP, 1987. Montreal Protocol on Substances that Deplete the Ozone Layer. Available at: http://ozone.unep.org/new_site/en/montreal_protocol.php.

Visteon UK, 2005. TIGERS. Available at: http://www.treehugger.com/cars/creating-electricity-with-exhaust-gas.html.

Wang et al., 2012. Fluid selection and parametric optimization of organic Rankine cycle using low temperature waste heat. *Energy*, 40(1), pp.107–115. Available at: http://linkinghub.elsevier.com/retrieve/pii/S036054421200117X [Accessed December 25, 2014].

Wang et al., 2011. Study of working fluid selection of organic Rankine cycle (ORC) for engine waste heat recovery. *Energy*, 36(5), pp.3406–3418. Available at: http://linkinghub.elsevier.com/retrieve/pii/S036054421100209X [Accessed August 20, 2014].

Wikipedia, Wikipedia. Available at: https://en.wikipedia.org/.

Woodland et al., 2012. Experimental Testing of an Organic Rankine Cycle with Scroll-type Expander.

Ziviani et al., 2012. Development and Validation of an Advanced Simulation Model for ORC-Based System.

Intentionally Blank Page

Appendix

APPENDIX I: NsDs results for 0,16 m of diameter

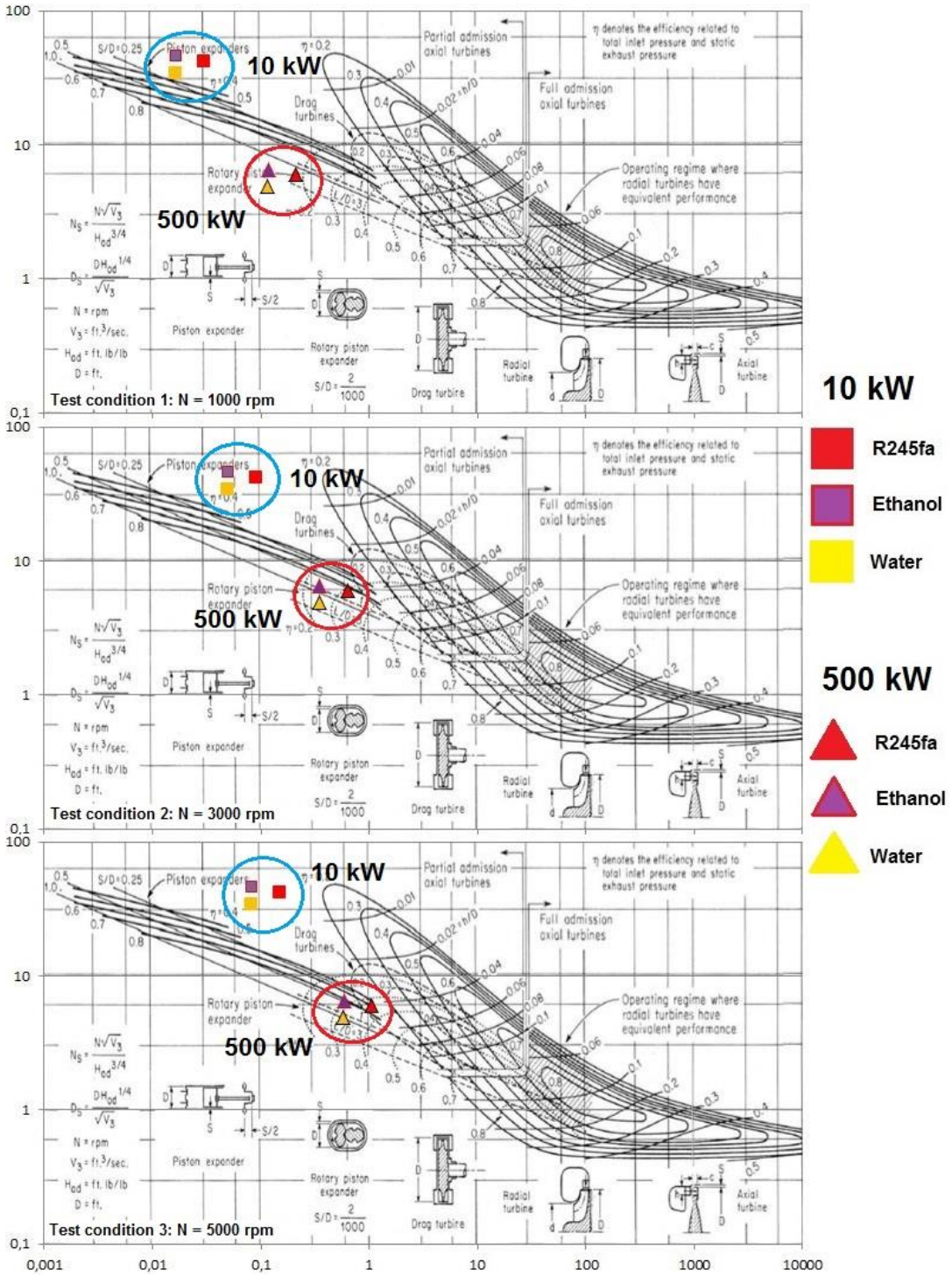

Appendix 1 - Top: Test condition 1; Center: Test condition 2; Bottom: Test condition 3 (see Table 3.2), corresponding to the displacement expanders rotary speeds and a diameter of 0,16 m

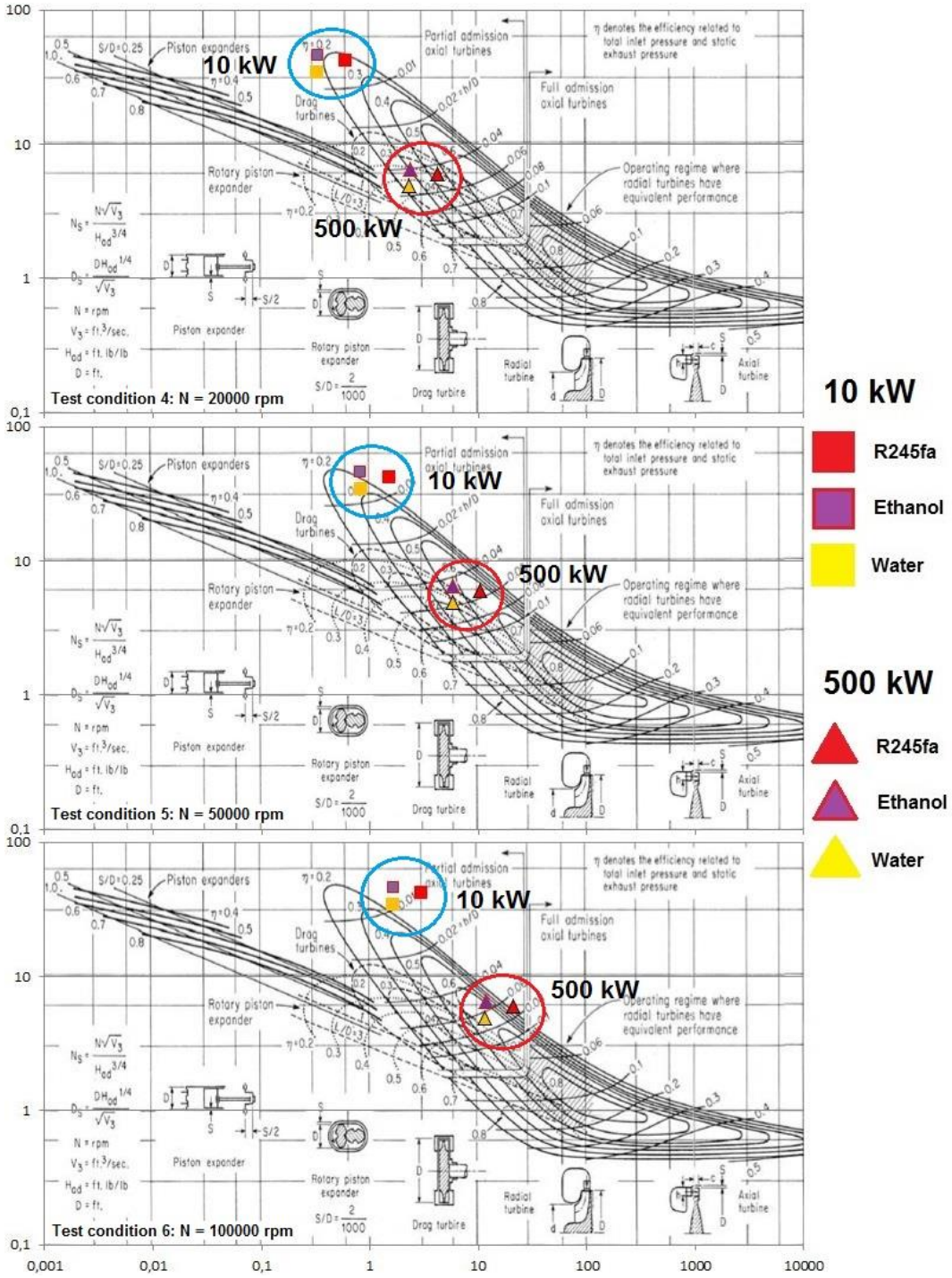

Appendix 2 - Top: Test condition 4; Center: Test condition 5; Bottom: Test condition 6 (see Table 3.2), corresponding to the turbine expanders rotary speeds and a diameter of 0,16 m

APPENDIX II: Extra libraries for AMESim

- **IFP Drive** – this library can be used to model a global vehicle, from the simple gasoline vehicle such as hybrid one (IFP stands for *Institut Français du Pétrole*);
- **IFP Engine** – it is used for the analysis of engine performance, fuel consumption and engine-out emissions as well as for the definition of plant models for control development purposes;
- **CFD 1D gas dynamics** – allows a significant improvement in simulation accuracy of gas flows in pipes and networks, and must be associated to the IFP-Engine, IFP-Exhaust or Pneumatic libraries (it is not a stand-alone library);
- **IFP Exhaust** – dedicated to the modeling of exhaust systems. It is possible to focus on the physics of the catalytic process but also to analyze the performance of the whole exhaust system in terms of thermal behavior and emissions;
- **Hydraulic** – contains general hydraulic components suitable for simulating ideal dynamic behavior based on component performance parameters. It is possible to apply this library to automotive, aerospace and industrial equipment applications, with the use of pumps, motors and orifices, and also special valves and complex models of pipes and hoses;
- **Discrete Partitioning** – this is an add-on for the **Hydraulic** library. It is a physical method to create parallelized models, and can be used to divide big hydraulic systems into smaller sub-systems, making it possible to run a simulation as a form of co-simulation, improving simulation times;
- **Hydraulic Component Design** – contains the basic building blocks of any hydro-mechanical system, in order to design detailed and more precise hydraulic components;
- **Hydraulic Resistance** – used to create large hydraulic networks and evaluate the evolution of pressure drops and flow rates through a hydraulic network;
- **Filling** – developed to evaluate the time needed to fill in an entire circuit and evaluate the order in which the different components of the network will be filled. Can be used for example to determine the time taken to fill the lubrication circuits of an engine with oil during startup;

- **Thermal** – used to model heat transfer between solid materials and to study the thermal evolution in these solids when submitted to different kinds of heat sources.
- **Thermal Hydraulic** – used to model thermal phenomena in liquids and to study the thermal evolution in these liquids when submitted to different kinds of heat sources and power sources.
- **Thermal Hydraulic Resistance** – ducts and other connection components for thermal systems, that are used to determine the evolution of pressure drops and flow rates in hydraulic networks in which variations of fluid temperature have a great influence on the overall behavior;
- **Thermal Hydraulic Component Design** – used to construct a model of a component, enabling the user to go very deep into the details of the component's technology;
- **Cooling System** – allows you to combine models for the cooling system, lubrication system, and exhaust system to study the complete thermal behavior of an engine. Can be used to compute the heat exchanged between the coolant and the exhaust gas flowing through the EGR;
- **Two-Phase Flow** – used for modelling thermo-hydraulic systems where there is a change of phase (liquid-vapor), like the ORC system of this work;
- **Air-Conditioning –** used to model steady state and dynamic behavior of air conditioning systems, and if can be used to compute the thermal balance of the moist air in a vehicle cabin;
- **Heat Exchangers Assembly Tool** – used to study heat exchanger interactions within a confined environment, such as under the hood for automotive applications (automotive radiator subpart is included in this library);
- **Pneumatic** – very extensive library with many different components to either model large networks or design complex pneumatic components through basic components like pneumatic valves, and can be used to observe the evolution of temperatures, pressures and mass flow rates in pneumatic systems. These systems can be part of areas such as automotive, railway, aerospace or industrial equipment;
- **Pneumatic Component Design** – contains the basic building blocks of any pneumatic-mechanical system, and can be used to design any kind pneumatic valve with detail, like actuators, compressors and dampers;

- **Gas mixture** – used to model systems using gas mixtures up to 20 species.
- **Moist Air** – contains a set of thermal-pneumatic and thermal-hydraulic components for modeling systems dealing with moist air;
- **Electrochemistry Components** – provides set of component submodels ready for use with existing components. It can be used in most engineering applications where flows of electrons and ionic species take place due to electrochemical reactions
- **Fuel Cell** – components for designing and optimizing the integration of fuel stacks inside fuel cell systems;
- **Powertrain** – used to model systems such as driveline or complete gearboxes, including vibration and loss effects;
- **Finite Element Import** – enables connection of 3D structural models from a FEM software to mechanical models;
- **Planar Mechanical** – used to model dynamics of bodies in two dimensions. It gives the possibility of connecting, for example, a rope to a rigid body, and study the dynamic effects of a mechanical action applied on it;
- **Vehicle Dynamics** – provides a huge amount of components that are used to design multi-body chassis, suspensions, tires, steering and braking systems;
- **Vehicle Dynamics iCar** – is used to model chassis, suspensions, tires, steering and braking systems which are connected to a graphical interface for parameters setting;
- **Cams and Followers** – used to model cams and followers.
- **Electro Mechanical** – contains elements such as air gaps, metal elements, magnets and coils to construct a magnetic circuit such as a solenoid or a dynamo. Contains dynamic effects such as hysteresis and electric properties;
- **Electric Motors and Drives** – used to model electric parts which replace mechanical and hydraulic actuation.
- **Automotive Electrics** – used to model automotive electrical components, such as window mechanism or head lamps;
- **Engine Signal Generator** – contains the elements that cover the generation of control signals for engines. Can generate a signal profile from an impulse;
- **Electric Storage –** contains components like battery packs, LiIon cell batteries and capacitors, in order to simulate high frequency phenomena;

- **Aeronautics & Space** – contains a set of basic components dedicated to Aeronautics and Space applications. It provides flight mission definition, atmosphere models, sensors and power generation models and is able to support a large number of applications providing the components allowing to assess system performance in realistic conditions. It also allows to link system simulation with engine desk through the NPSS interface.
- **Aircraft Electrics** – provides a set of applicative components which allow the user to model aerospace electrical systems. Electrical Power Generation and Distribution Systems such as generators and transformer rectifier units can be modeled;
- **Aircraft Fuel System** – it provides components dedicated to fuel system applications, such as tanks with variable shape with liquid and pneumatic gas or gas mixture for inertial applications, specific orifices models and gauge models. The tank can be moved in space and submitted to accelerations in order to compute the liquid movements;
- **Electrical Static Conversion** – this library provides the main functions of power electronics in one click, making it easy to build converters (for example inverters or rectifiers);
- **Electrical Basics** – contains current, voltage and power sources, ampermeters, voltmeters and potentiometers, and combined with the Electrical Static Conversion library it provides an effective solution to supply a motor, a linear transducer of or to convert the energy form of an electric network;
- **Generic Cosimulation** - allows the creation and configuration of specific interface blocks that can be used to sketch and perform Hybrid Co-simulation.